PROCESS ANALYSIS AND DESIGN FOR GRINDING ROBOT TOOL HOLDERS

by

NEIL GOLDFINE

B.S., Mech. Eng., University of Pennsylvania
B.S., Elec. Eng., University of Pennsylvania
(1982)

SUBMITTED IN PARTIAL FULFILLMENT
OF THE REQUIREMENTS OF THE
DEGREE OF

MASTER OF SCIENCE
IN MECHANICAL ENGINEERING

at the

MASSACHUSETTS INSTITUTUE OF TECHNOLOGY

January 1985

Signature of Author.....
Department of Mechanical Engineering
January 18,1985

Certified by.....
Haruhiko Asada
Thesis Supervisor

Accepted by.....
Ain A. Sonin
Departmental Committee on Graduate Studies, Chairman
Department of Mechanical Engineering

PROCESS ANALYSIS AND DESIGN FOR GRINDING ROBOT TOOL HOLDERS

by

NEIL GOLDFINE

Submitted to the Department of Mechanical Engineering
on January 18, 1985 in partial fulfillment of the
requirements for the Degree of Master of Science in
Mechanical Engineering

ABSTRACT

A simple and effective solution to the robot grinding problem is introduced, which significantly reduces vibrations during grinding without additional actuators or active control. The objective is to determine the optimal compliance design for grinding robot tool holders. Specifically, the tool holder design should improve accuracy and productivity while protecting the robot arm from the large unpredictable forces which are inherent in the grinding process.

It is found that the degree of correlation between the dynamic behavior of the wheel in the directions normal and tangent to the desired workpiece surface has a direct effect on the grinding performance. This fact is utilized to determine the optimal tool holder compliance design through analysis, simulation and experimentation. The resulting design conclusions have been incorporated in two different end-effectors which have been tested on the grinding of weld seams.

Thesis Supervisor: Dr. Haruhiko Asada

Title: Assistant Professor of Mechanical Engineering

To my parents

Beatrice and Leonard Goldfine

ACKNOWLEDGEMENTS

I would like to thank Dr. Haruhiko Asada for providing constant guidance and insight during this research. I would also like to thank Dr. George Chryssolouris for his useful comments on grinding process modeling. In addition, I would like to thank Kamal Youcef-Toumi for his comments and technical assistance and Mark Bouchard for assistance with experimentation.

Table of Contents

		page
	TITLE	1
	ABSTRACT	2
	DEDICATION	3
	ACKNOWLEDGEMENTS	4
	TABLE OF CONTENTS	5
	LIST OF FIGURES	7
	LIST OF SYMBOLS	9
1.	INTRODUCTION	10
2.	DYNAMIC BEHAVIOR OF GRINDING MACHINES	
	2.1 Background in Grinding Machine Dynamics	13
	2.2 Stability and Chatter During Grinding	16
	2.3 Static and Dynamic Stiffness Measurement	22
	2.4 Models for Specific Grinding Applications	24
3.	PROCESS ANALYSIS FOR GRINDING WITH ROBOTS	
	3.1 Important Issues in Grinding with Robots	33
	3.2 Grinding Force Analysis	34
	3.3 Modeling and Characterization of Tool Suspension System	39
4.	SIMULATION OF GRINDING WITH ROBOTS	
	4.1 Performence Measurement	47
	4.2 Worst Case	49
	4.3 Effect of Correlation on Grindig Performance	49
	4.4 Effect of Structure Orientation Angle	53

5. GRINDING EXPERIMENTATION

5.1 Setup and Procedure 56
5.2 Comparison with Simulation 56

6. END-EFFECTOR DESIGN AND IMPLEMENTATION

6.1 Design Objectives 68
6.2 Determination of Tangential Compliance Characteristics 69
6.3 Implementation 74

7. CONCLUSION 78

REFERENCES 79

LIST OF FIGURES PAGE

1. Relative importance of dynamic instability 31

2. Grinding Process Model 35

3. Model of Robotic Grinding Process 40

4. Effect of design parameters α and d on κ 45

5. Definition of (a) Y_{max} for $y_0 = 0$, $x_0>0$ and (b) t_s for $0<y_0<s_0$, $x_0 = 0$. 48

6. Simulated phase plane plots for (a) $x_0 = 0.1$ in, $y_0 = 0$ and (b) $x_0 = 0$, $y_0 = 0.1$ in. 50

7. Simulated effect of directional stiffness properties K_t/K_n ($= \kappa\tan\theta$) on Y_{max}/x_0 and t_s for $y_0 = 0$, $x_0 > 0$ 51

8. Simulated effect of directional stiffness properties K_t/K_n ($= \kappa\tan\theta$) on Y_{max}/x_0 and t_s for $0 < y_0 < s_0$, $x_0 = 0$ 52

9. Simulated effect of α on Y_{max} for $x_0= 5\text{x}10^{-3}$ in and $y_0=0$ 54

10. Photographs of experimental setup 57

11. Comparison of (a) experimental and (b) simulated grinding data for $\alpha = -45^\circ$ and $k_q = 10k_p$. 59

12. Experimental grinding data 60

13. Experimental effect of α on Y_{max} and Y_{avg} for $x_0 = 5\text{x}10^{-3}$ in and $y_0 = 0$ 66

14. Effect of tangential compliance on grinding behavior for (a) $K_t = K_n$ (b) $K_t = K_n/100$ (c) $K_t = K_n/1000$ and (d) $K_t = K_n/5000$ 70

15. American Robot and end-effector photographs 75

16. Daikin Robot and end-effector photographs 77

LIST OF SYMBOLS

b_p	damping in p direction
b_q	damping in q direction
B_n	damping in normal direction
B_t	damping in tangential direction
C	grinding force constant
C_t	tangential grinding force constant
C_n	normal grinding force constant
F	resultant grinding force
F_t	tangential grinding force
F_n	normal grinding force
f_p	grinding force in p direction
f_q	grinding force in q direction
k_p	spring constant in p direction
k_q	spring constant in q direction
K_n	spring constant in normal direction
K_t	spring constant in tangential direction
m	mass of grinding tool
O	origin of Oxy and Opq reference frames
p	deflection along principal axis p
q	deflection along principal axis q
s_0	desired depth of cut
t_s	vibration decay time constant
v_0	desired feed rate
x	deflection along x axis (tangential deflection)
x_0	initial deflection in x direction (tangential)
y	deflection along y axis (normal deflection)
y_0	initial deflection in y direction (normal)
Y_{max}	maximum deflection in y direction

Y_{avg}	average deflection in y direction
Y_{ss}	steady state deflection in y direction
Z	volume removal rate
Z_w	workpiece volume removal rate

α	structure orientation angle
Λ_w	Metal Removal Parameter
λ	geometric constant
μ	grinding force coupling coefficient
κ	correlation coefficient
θ	resultant force angle

1 INTRODUCTION

The application of robot manipulators to surface machining processes, such as grinding of weld seams and deburring of castings, has received considerable attention in recent years [1,2,3]. These tasks have remained highly labor intensive in industry despite low productivity, high costs and hazardous working environments. Although robots appear to be suitable for these tasks, present day robots have several technical problems that have prevented their successful application.

In grinding applications, the robot manipulator is required to locate and hold the grinding tool in the face of large, vibratory forces which are inherent in the grinding process. Exposure to these unpredictable loads generally results in large deflections at the tip of the robot arm. These deflections degrade the process accuracy and the surface finish. In addition, the large vibratory loads may cause damage to the robot's mechanical structure.

In conventional machine tools, large deflections are eliminated by designing for maximum stiffness in the whole structure [4]. Unfortunately, it is not feasible for robot manipulators to have such high stiffness. Robots are generally required to meet demands for wide workspace, dexterity and mobility with many degrees of freedom. For many robot applications including surface grinding these demands introduce kinematic constraints which make robots unavoidably poor in

structural stiffness compared to conventional machine tools.

As an alternative to high stiffness design, active feedback control has been applied to grinding robots for reducing dynamic deflections. Kuntze [5] proposed an active control scheme, in which the actuators are commanded to increase torques in the opposite direction of the deflections. These methods reduce dynamic deflections in a certain frequency range. Generally, it is difficult for these control schemes to perform well over a wide frequency band because they must drive the entire, massive robot arm.

Actively controlling wrist joints or local actuators which are located near the tip of the arm is easier and more effective than moving the whole arm, because the inertial forces are smaller. Paul [6] applied an active isolator to a chipping robot, where the isolator attached to the arm tip reduces the vibrations seen by the robot. Sharon and Hardt [7] developed a multi-axis local actuator, which compensates for positioning errors at the end point, in a limited range.

For certain applications the stiffness of the robot can be significantly increased by directly contacting the workpiece. Asada, West [8], and Asada, Sawada [9] developed tool support mechanisms which couple the arm tip to the workpiece surface and bear large vibratory loads. These mechanisms allow the robot to compensate for the tolerancing errors of the workpiece, as well as to increase the stiffness with which the tool is held. Moore and Hogan [10] also

applied a local support mechanism to a drilling robot for part referenced positioning.

Thus, a number of methods for improving performance and positioning accuracy have been developed, which can be used for a variety of machining applications. A key to successful application, however, is a sound understanding of the machining process, specifically the dynamic interactions between the tool and the robot manipulator must be investigated. The grinding process, in particular, is a complicated dynamic process in which nonlinear dynamic behavior has a direct effect on the surface finish and accuracy.

In this research, the grinding process is investigated through analysis, simulation and experimentation. The relation between the tool vibration and the stiffness with which the tool is held is evaluated, and the optimal tool holder compliance is determined. A simple and effective solution to the robot grinding problem is found, which significantly reduces vibrations without additional actuators or active control.

2 DYNAMIC BEHAVIOR OF GRINDING MACHINES

2.1 Background on Grinding Machine Dynamics

The application of robots to machining tasks is a relatively new problem, hence, limitted process analysis is availabe for grinding robots. However, the analysis of the dynamic behavior of grinding machines has recieved considerable attention and a wealth of knowledge is available on this subject. Unfortunately, most current research in grinding with robots has concentrated on controlling the robot in the face of unknown forces and vibrations. Of course, this research is necessary, but before the robot can be controlled in an efficient and effective manner, the robot grinding process itself must be analysed. Based on this analysis the most effective control variables, control strategy and mechanical design can then be determined. In this research, the determination of the optimal end-effector mechanical design is the central goal.

The dynamic behavior of grinding machines is inherently complex. Although many prominent researchers have studied grinding dynamics, much of the behavior commonly observed in experiments and practice has not yet been modelled in a complete manner. The grinding process appears to be similar in many ways to other common cutting processes [11], however, the cutting edges, in grinding, are of varied and indeterminate geometry, and the cutting properties of the grinding wheel change more rapidly than in other cutting

processes [4,11]. As a result, grinding process dynamics are extremely nonlinear and difficult to model.

Although no complete model of grinding machine dynamics has been developed, a strong foundation of physical understanding, theory and practical knowledge has been established by prominent investigators such as Shaw [11], Tobias [4], Doi [12], Hahn [13], Konig [14], Lindsey [15], Peters [16], Polacek [17], Saini [18], Salje [19], and Snoeys [20]. The objective of this section is to provide a summary of the accomplishments of these and other investigators, and to develop an understanding of the major issues and problems involved in evaluating and improving dynamic behavior during grinding.

Many researchers have derived expressions for the grinding force. Hahn and Lindsay [13,15] and several other investigators have developed empirical relations which have become the basis of most grinding process models. In section 3.1, a summary of accomplishments in grinding force analysis is presented and a aggregate expression for the grinding force is developed from empirical relations.

The elimination or reduction of chatter during grinding is the ultimate objective of most research in grinding dynamics. Hence, the first major issue discussed in this chapter is the stability of the grinding process, with emphasis on the nature and causes of regenerative chatter.

It is not possible to completely cover all physical phenomenon involved in grinding machine vabrations. However, it has been found by Kumar and Shaw [26] that although thermal effects, lubrication and other peripheral phenomenon play an important role in grinding dynamics, thermal effects are neqligible compared to mechanical effects for certain typical applications. Thus, research concerning the static and dynamic deflections of the grinding wheel resulting from mechanical effects such as wheel imbalance, dynamic coupling and the development of waves on the grinding wheel are emphasized in this research [21-26].

It has also been found that a primay parameter in most theoretical models of grinding dynamics is the compliance of the wheel-work contact area [20]. As a result, much of the research in grinding dynamics has concentrated on the measurement of static and dynamic stiffness properties in the contact area [27-32]. A survey of recent research on static and dynamic stiffness measurement is presented in section 2.3.

It is also helpful to discuss the practical application of theory and physical understanding to actual applications. Several models of dynamic behavior have been presented for specific grinding applications such as internal [33-36], centerless [37,38], creep-feed [39,40], constant-load heavy [41], precision [42-44], profile [45], cylindrical plunge [19,25], surface [46], snag [47] and robotic grinding [48,49]. A brief discussion of the emphasis and

accomplishments of each of these models is provided in section 2.4. From this survey it is found that the importance of dynamic stability and other issues in grinding process analysis varies dramatically for different processes.

2.2 Stability and Chatter During Grinding

As stated earlier, the complexity of the grinding process has prevented the development of a complete process model. For this reason the causes and nature of vibrations during grinding are not completely understood. However, insight and knowledge about stability and chatter during grinding has been obtained through analysis and experimentation. In this section, some of the accomplishments of past research in this area are summarized. The goal is to establish the level of current understanding and to provide a basis for further research and development.

In most recent investigations of grinding chatter some reference to waviness (surface waves) on the grinding wheel and workpiece surfaces is made. Many researchers [21-26] agree that the occurance of surface waves is of central importance in evaluating grinding chatter. The occurance of waves on the wheel and workpiece is directly associated with the relative vibrations of the grinding wheel [23]. These vibrations are generally divided into three groups [17,23,25]:

1. Forced vibrations are caused by external excitation forces. In grinding processes the most common source of forced vibration is the wheel unbalance, and the number of waves formed on the workpiece periphery is often proportional to the rotational speed of the spindle.

2. "Passive" vibrations are transmitted through foundations from other machines or caused by random variations in the workpiece material. These vibrations are generally classified as forced, however, their identification is often much more difficult.

3. Self-excited vibrations (chatter) results from the cutting action itself, without the presence of external periodic forces. These vibrations often result in the occurance of waves on the grinding wheel circumference, and these waves tend to grow as the process progresses.

The term regenerative chatter was originally introduced by Tobias and Fishwick in 1956 and Hahn in 1959 [23]. Many physical explanations for regenerative chatter have appeared in the literature since that time. For example, one commonly accepted cause of chatter in grinding is chip thickness variation between successive cuts. Many researchers have formed lists of physical effects and possible causes of regenerative chatter in order to establish the current state of understanding and accomplishment [17,21,23]. From the work of these and other investigators a list of interesting physical phenomenon associated with grinding chatter is compiled.

1. For most metal cutting processes the growth rate of chatter is high and the stability boundary is the limit of acceptable performance. However, in grinding the growth of instability is often slow and acceptable grinding performance may be achieved long after the stability boundary has been passed [21]. In fact it has been shown that a significant number of grinding operations generally perform

under unstable conditions [22].

2. Undulations on the workpiece surface often occur when the grinding wheel moves periodically relative to the workpiece. However, the generation of these undulations is only possible if the contact length of the interaction zone is smaller than the wave length on the workpiece surface. If the vibration frequency is very high or the workpiece speed is very slow the surface will not be modulated even for large amplitudes of the applied dynamic force [31].

3. The occurance of waviness is of primary importance when over-soft wheels are used and these waves are the dominant influence on the dynamic stability of the grinding process. Also the worn grains will not detach themselves if the wheel is too hard. Furthermore, small chips of the workpiece material remain lodged between the grits; this shows up as glazing of the wheel surface. Hahn [13] has shown that this loading of the surface can occur in a very short time and will take place in an uneven manner if vibrations occur. Although the quantity of material adhering to the surface may be small the resulting waviness will tend to grow and expanding oscillations will generally result [4].

4. When vibrations of the grinding machine structure occur the vibration amplitude for the element with the lowest stiffness is the largest. These elements include the workpiece, the grinding wheel, the spindle, and all other elastic members of the machine structure. This large amplitude vibration produces a modulating effect [23].

5. The compliance of the wheel-work contact area is a basic parameter which has a direct effect on the stability requirements in grinding [22].

This is in no way a complete list of physical effects and causes of grinding chatter. The purpose of the list is to provide an introduction to some important issues to be considered in modelling and evaluating chatter in grinding.

Several different approaches to modeling the dynamic behavior of grinding

machines have appeared in the literature, such as feedback, kinematics and numerical methods [24]. One approach which provides excellent physical insight into the relation between important mechanical properties is the feedback approach. Snoeys and Wang [31] have presented an extensive feedback model of the grinding process. Some basic conclusions which resulted from the analysis presented by Snoeys and Wang are:

1. Grinding stability is worse for higher contact area stiffness. The compliance of the grinding wheel depends on the characteristics of the grinding wheel, thus, fine grit sizes and gentle dressing conditions are a disadvantage and soft wheels with small E modulus values are preferable.

2. Higher grinding forces produce larger values of contact stiffness. Some results of this effect are that stability is improved for high wheel speed, small work speeds, sharp cutting edges, etc. and that a decrease of stability results for dull cutting grains and high stock removal.

3. Acceptable grinding performance is often obtained during unstable conditions because the building up of self-excited vibrations is generally very slow.

4. Forced vibrations are not always detrimental to the stability of the process, since in certain cases vibrations can yield a decrease of the contact stiffness and will tend to stabilize the cutting operation.

5. As an " extremely simplified stability criterion " the static stiffness of a grinding wheel may be estimated by 2×10^6 lb/in for each inch of the grinding wheel width.

It is clear from these conclusions that the contact stiffness will play an important role in the dynamic behavior of the grinding machine. For this reason the determination of the relationship between the static and dynamic

loads and the contact stiffness has recieved considerable attention. In section 2.3, some techniques for determining this relationship are discussed.

Some interesting results derived from several different theoretical models for grinding process dynamics are now discussed. Pahlitzsch and Cuntze [25] found a somewhat contradictory result to that shown by Snoeys and Wang [31] for the effects of wheel hardness. They agree with Snoeys and Wang that harder grinding wheels excite more, but they also note that softer grinding wheels wear faster. As a result, they find that the smallest temporal rise of chatter amplitude and the longest redress life are to be expected for grinding wheels of mean hardness.

Pahlitzsch and Cuntze [25] also found that the excitation of the workpiece by the waviness of the grinding wheel is only possible if the grinding wheel is sufficiently hard. A soft grinding wheel will break out when exposed to the variations in pressure resulting from vibratory loads, and predominant waves on the grinding wheel surface can not develop. This statement does not agree with statement (3) above and some disagreement on this point exists throughout the literature.

It has been found by Sexton and Stone [24] that the tradeoff between the good effect of high wheel hardness on wheel wear and its negative effect on grinding stability can be avoided by increasing the radial flexibility of the wheel while maintaining high values of the wheel's natural frequency and damping.

Hence, they are of the opinion that "ultra-hard abrasives will now assume their rightful place as the abrasive for the future."

Polacek [17] presents some interesting effects of important process parameters on the process stability. He begins with the relationship P = -br(Y-Yo), where P is the cutting force, b is the chip width, r is the "coupling coefficient" as defined in this equation and (Y-Yo) is the actual depth of cut. For a single degree of freedom system he finds that for a particular frequency ω_{kr} of forced vibrations or self-excited vibrations the amplitude of the vibration will increase at a maximum value. He also finds that in a given range of frequencies about this point the process is unstable while outside this range the process is stable.

The physical explanations of grinding chatter discussed in this section represent a brief survey of the state of current knowledge on grinding dynamics. It is clear from this survey of research that a complete description of grinding machine dynamics is not yet available and a great deal of research is necessary before such a description will be developed. In chapters 3 and 4 an aggregate approach to modeling and simulating dynamic behavior in grinding for robotic applications is presented. The purpose is to develop a model of the process which can generate behavior similar to that observed in experimentation and practice.

2.3 Static and Dynamic Stiffness Measurement

The significance of local elastic deflections in grinding has been recognized by both research workers and industrial practitioners. Geometrically, the local contact deflections influence both the dimensional accuracy of the workpiece and the resulting surface finish [27].

The static and dynamic deflections during grinding depend directly on the static and dynamic stiffness of the grinding wheel and the grinding machine structure. Some contraversy exits, however, in determining the static stiffness of the grinding wheel as a function of the static load. Nakayama, Breker and Shaw [28] found that individual grain deflections vary as $P^{2/3}$, where P is the static load on an individual grain. According to Hahn [29] these results are not in agreement with wheel contact stiffness results obtained by Hahn and Price [30] using the contact resonance method.

In the contact resonance method [30] a small test mass, having a 1/8 in. diameter tungsten carbide tip is pressed against the dressed periphery of a grinding wheel and driven vibrationally to find the contact resonant frequency. This resonant frequency provides an estimate of the local contact stiffness. Hahn and Price [30] found that

$$\omega_n \simeq P^{1/4}$$

and this implies that the stiffness varies as $P^{1/2}$, thus

$$dp/ds \simeq P^{1/2}$$

This is then integrated and leads to the conclusion that the stiffness varies as $P^{1/2}$ and not $P^{2/3}$. The difference between these results is explained by Shaw. He states that in the experiments run by Hahn and Price several grains are contacted and the results include the effects of variation in the number of grains in contact with the loading tool as well as the deflection of individual grains. Thus, Shaw believes that the static loading of individual grains provides a more accurate measure of grinding wheel stiffness.

This disagreement on the relationship for static wheel stiffness shows that the fundamental properties of grinding wheels are not completely understood and no generally accepted relation for the nonlinear variation of the grinding wheel stiffness with the static load exists.

Unfortunately, it is even more difficult to measure the contact stiffness during grinding. One method for obtaining an estimate of the order of magnitude of the compliance of the contact area during grinding is to eliminate the relative motion of the workpiece in the tangential direction[31].

It is also important to measure the static and dynamic deflections of the grinding wheel and the machine tool structure directly. An innovative method for the experimental determination of deflections during grinding was presented by Brown, Saito and Shaw [32]. This method utilizes a patch grinding technique to seperate the local deflections from the general deflections of the machine frame and the grinding wheel spindle.

One goal for understanding the nature of deflections in grinding and for determining the static and dynamic stiffness of grinding wheels is to provide estimates for stiffness parameters which can then be introduced into theoretical models of grinding process dynamics. In the next section, a survey of models for some specific grinding applications is presented.

2.4 Models for Specific Grinding Applications

The practical application of theory and physical understanding to actual grinding applications is the ultimate goal of all research in grinding machine dynamics. In this section, a survey of models for specific grinding applications is presented. It is also found that the major issues in robotic grinding are quite different than those in many more conventional grinding applications.

First, the internal grinding application is discussed. Several models of this process have been presented [33-36]. In a paper by Hahn and Lindsay [34] practical working equations are derived from a model of the internal grinding process and these equations are used as a basis for optimizing grinding cycles. Hahn and Lindsay begin with the empirical relation $Zw = \Lambda_{wc}(Fn-Fpc)$, where Zw is the material removed from the workpiece by cutting, Λ_{wc} is the "cutting metal removal parameter", Fn is the normal grinding force and Fpc is the ploughing-cutting transitional force intensity. The term Fpc represents the force level required to begin chip formation. From this equation and a similar

equation for the material removed during ploughing a model of the internal grinding process is developed. Hahn and Lindsay then identify several critical parameters in the optimization of internal grinding cycles.

A paper presented by Kel'zon and Guk'yamkhov [36] also presents a model of the internal grinding process. The central theme of this paper is the determination of the effects of elastic supports on grinding stability and performance. The authors indicate the effect on machined surface quality of forced vibrations of the spindle on two elastic supports, resulting from the static and moment-induced unbalance of the rotor and by a cutting force, which is variable in time. From the data obtained they find it possible to predict the machining accuracy on the basis of theoretical calculations.

The centerless grinding process has also recieved a significant amount of attention in grinding research. In the centerless grinding process the geometrical configuration and orientation of the machine tool plays an important role in process stability [37,38]. In an article presented by Richards, Rowe and Koenigsberger [38] geometric stability charts are developed and their usefulness is validated through extensive experimentation. The authors conclude that:

1. Theoretical geometric stability should be considered in order to avoid highly unstable operating conditions. Stability charts are easy to compute and provide necessary information that facilitates the interpretation of the grinding results. In particular it is possible to distinguish between geometric instability and dynamic chatter from these charts.

2. Resonant frequencies of the machine should be as high as possible to minimize the tendancy towards large amplitude waviness.

3. Close proximity between resonant frequency and a geometrical instability does not always constitute an unfavorable condition.

Other articles presented on this topic provide models of various effects such as frictional damping [37] which can be utilized to improve grinding performance.

The next process discussed is creep-feed grinding. Trimal [39] presents an interesting comparison between creep-feed and conventional grinding. In this article an attempt is made to explain the differences between creep-feed and conventional grinding on the basis of equilibrium of attritious and fracture wear of the wheel surface. It is found that this equilibrium depends on the conditions at the wheel-work interface. Some conclusions of this analysis are:

1. Creep-feed grinding provides a considerable reduction of out of contact time which can reach as high as 90% of the total time in conventional surface grinding. This advantage is lost in cylindrical applications making it harder for the creep-feed technique to prove attractive for this application.

2. The creep-feed technique offers substantially better form holding. This phenomenon does not seem to be caused primarily by the elimination of shock load of the wheel surface by repeatedly coliding with the edge of a component but by conditions at the interface of the wheel and workpiece. Thus, this advantage should still hold for cylindrical creep-feed grinding.

3. The reduction of wheel speed appears to have a very benificial effect and should be investigated in more detail.

4. Conditions at the interface such as force per grit and temperature determine the equilibrium of attritious and fracture wear of active grits, and this equilibrium can explain all special features of creep-feed grinding.

Constant load heavy grinding has wide application in such jobs as steel snagging, foundry deburring, turbine parts machining etc.[41]. In a paper by Matsuo, Matsubara and Kumamoto [41] the effects of varying load, traverse speed, wheel width and wheel type were studied from the stand-point of metal removal rate, wheel wear, grinding ratio, grinding force and surface roughness with special attention to grinding temperature. Some conclusions of this article are:

1. Wheel width does not affect the metal removal rate and wheel wear rate if load is identical.

2. The tangential force increases linearly with increasing removal rate, regardless of traverse speed, wheel width, and wheel type. However, a wider workpiece causes a larger tangential force for the same removal rate.

3. The ground surface roughness is largely affecten by the wheel type

4. The grinding temperature ranges from 700°C t0 1200°C.

In precision internal and cylindrical grinding, the force between the wheel and work at which cutting can no longer occur is called the threshold force [42]. Hahn [42] finds that these forces often result in size errors, out of roundness of the workpiece, changes in surface finish and contour errors in cam grinding. Hahn presents a model for internal precision grinding in which he

discusses the effects of wheel speed, wheel and workpiece curvature, workpiece material, wheel type and coolant on grinding performance. He then derives the optimum feed rates for rounding up of eccentricities and for reducing workpiece errors. In a paper by Lindsay and Hahn [43] the sparkout behavior in precision grinding is discussed and modeled. In a second paper by Hahn [44] he discusses and models regenerative chatter in precision grinding operations. He finds a model of regenerative chatter can be derived directly from the simple proposition that the instantaneous depth of penetration of the wheel into the work is proportional to the instantaneous dynamic force existing between wheel and work. He also finds that this model can predict a spectrum of values for the cycles of vibration per revolution of work for which the process should be stable.

The profile grinding process is discussed by Salje [45]. He finds that, when asymmetrical profiles are ground, axial forces on the grinding wheel cause deformation of the wheel in that direction and the ground profile is inaccurate. Another problem discussed in his paper is the variation of surface roughness over the profile for the different dressing conditions and the different plunge angles used in angular plunge grindng. He finds that the right dressing conditions and plunge angle must be selected to avoid chatter or burn marks on the workpiece.

The dynamic behavior of surface grinding machine structures is modelled

in an article by Kudinov [46]. Using the model he determines the following methods for improving the dynamic behavior.

1. Increasing the stiffness if the spindle taper, grinding wheel faceplate, the grinding head front wall and also the vertical feed mechanism.
2. Mounting the wheel-drive electric motor without rubber shims
3. Dynamically balancing the mounted grinding wheel.

From this survey of process models it appears that major issues such as contact area stiffness and wheel imbance must be considered for most grinding applications. It is also apparent that dynamic instability is a major cause of instability in processes which are characterized by relatively low structural stiffness. Table 1 provides a summary of these and other major issues in the modelling of specific grinding applications.

From this table it is apparent that dynamic instability, which often results from the coupling in the grinding process [4], is only a major issue in grinding tasks which are characterized by relatively compliant structures. For example, in internal grinding the kinematic and geometric constraints of the process make relatively high compliance unavoidable. It was shown by Asada and Goldfine [48] that this is also true in robotic grinding. The relative importance of dynamic instability for several different applications is shown in Figure 1.

From this figure it is clear that in those tasks, such as creep-feed grinding and constant load heavy grinding, in which it is possible to design very stiff

TABLE 1

application \ issues	grinding cycle optimization	initial contact	wheel imbalance	geometric instability	structure compliance	wheel and contact area stiffness	dynamic instability	thermal effects
Internal	●	◒	●	—	●	●	●	◒
Centerless	●	◒	●	●	◒	●	◒	◒
Creep-feed	—	O	●	—	◒	●	O	●
Constant Load-Heavy	—	O	●	—	◒	●	O	●
Profile	◒	◒	●	—	◒	●	◒	◒
Cylindrical Plunge	●	O	●	—	◒	●	O	●
Surface	—	O	●	—	◒	●	◒	◒
Robotic	◒	●	●	—	●	●	●	◒

● major issue

◒ important issue

O minor issue

— not applicable

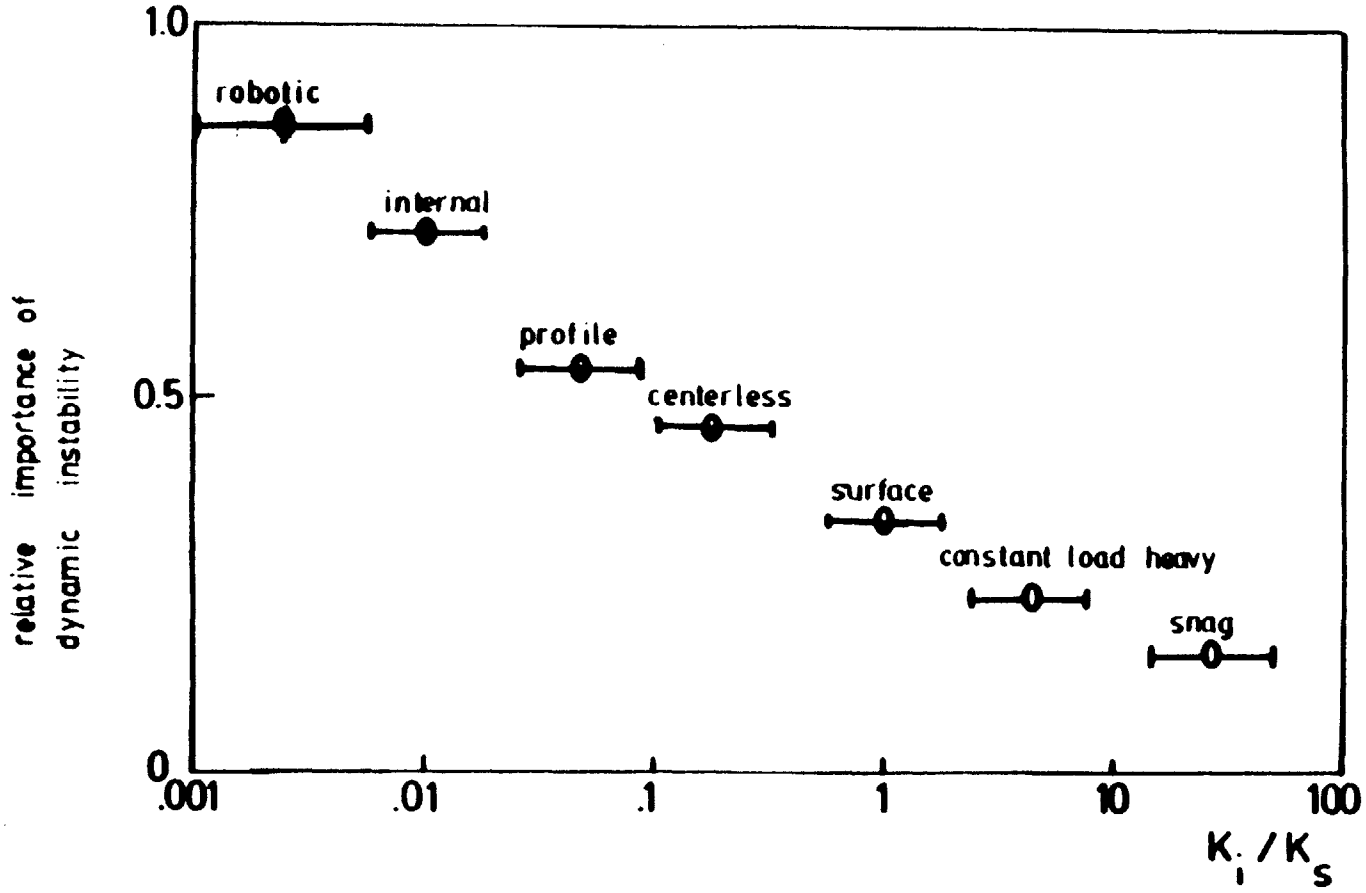

FIGURE 1: Relative importance of dynamic instability

machines, dynamic instability is not a major problem. However, the demands for wide workspace, adaptability and dexterity in many grinding applications introduce additional compliance which makes it difficult to attain high stiffness levels. Furthermore, it is difficult to maintain high stiffness levels in automated grinding machines without compromising flexibility and adaptability. Consequently, other means for reducing dynamic instability are necessary [48,49]. For this reason the elimination of dynamic instability resulting from coupling is the central theme of this research.

3 PROCESS ANALYSIS FOR GRINDING WITH ROBOTS

3.1 Important Issues In Grinding with Robots

As discussed in the previous section the major issue in grinding with robots is the elimination of dynamic instability. This is important because demands for wide workspace, high mobility and dexterity have made high compliance unavoidable in existing robot manipulators. It will be shown in the following sections that the directional stiffness properties of the tool holder have a significant effect on the process performance and stability.

Another characteristic of the grinding process which makes modeling the dynamic behavior difficult is the importance of nonlinear effects. In experimentation and practice, nonlinear behavior such as limit cycles with beats or modulation are commonly observed [17,31,48]. The best available method for evaluating the stability and performance of this nonlinear system is simulation. Although much physical understanding has been obtained from linear models [17,31] the major effects of chatter during grinding are not included in such models.

3.2 Grinding Force Analysis

In this section a macroscopic representation of the grinding force is derived from basic empirical relationships. The goal is not to model the process at a microscopic level but to develop an aggregated representation of the grinding force. The grinding process is represented schematically in Figure 2. The grinding wheel, in this model, is a flat cylindrical disk with a diameter much larger than the desired depth of cut, s_0.

The x axis, in the figure, is directed tangent to the desired workpiece surface, while the y axis is normal to this surface. The origin O is coincident with the center of the wheel, when the wheel is not deflected from its desired position. As the grinding process proceeds, the Oxy coordinate frame moves at the desired feed rate v_0. The deflections of the wheel are denoted by x(t) and y(t) and they are defined, with reference to the Oxy reference frame, to be positive when directed away from the workpiece. The variations of the wheel velocity in the x and y direction from the desired velocities are represented by $\dot{x}$ and $\dot{y}$.

As shown in Figure 2, the reaction force **F** acts upon the wheel during the grinding process. The reaction force has components in both the normal, y, and tangential, x, directions [50,51]. The coupling between the normal and tangential grinding forces has been assumed constant by many investigators.

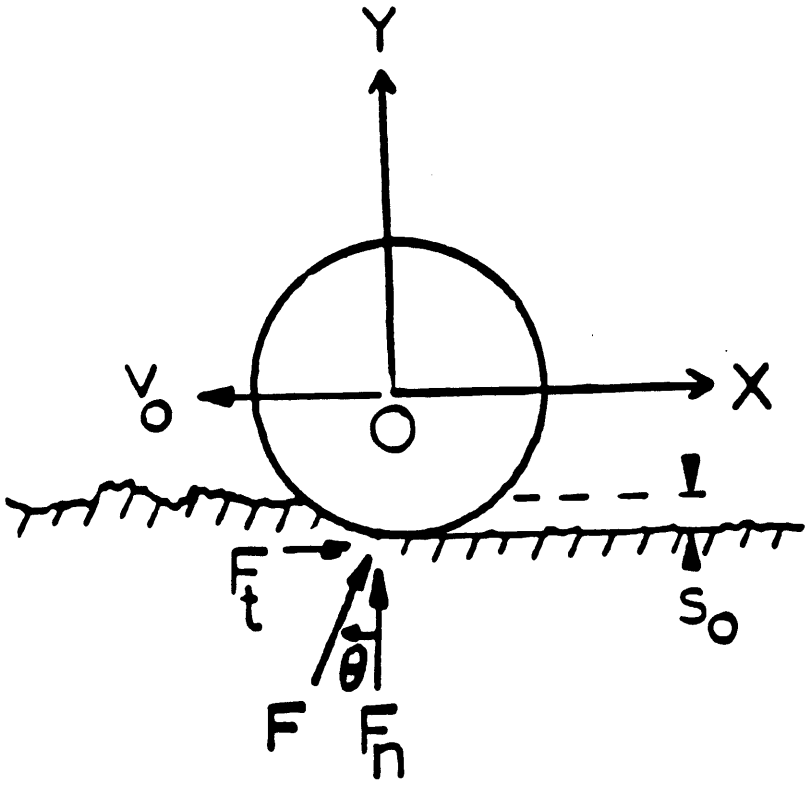

FIGURE 2: Grinding Process Model

This is similar to assuming a constant force angle θ. The resulting relationship is given in equation (1).

$$F_t = \mu F_n , \qquad \mu = \tan\theta \tag{1}$$

where μ is similar to a friction coefficient and is assumed constant.

The second important empirical equation is [50,51]

$$\begin{aligned} Z_w &= \Lambda_w F_n \\ F_n &= CZ , \qquad C = 1/\Lambda_w \end{aligned} \tag{2}$$

In the first equation above, the variable Z_w represents the volume removed from the workpiece surface. In addition to this volume removal term, the material removed from the wheel is often considered. However, it will be assumed here that the robot can sense the actual diameter of the wheel and adjust its desired position accordingly. Λ_w is the "Metal Removal Parameter" [51]. Since only the workpiece material removal is considered, Z_w is replaced by Z and the equation is rewritten as in the second equation (2).

In conventional grinding machines, the structure stiffness is high in every direction and it can be assumed that x, y, $\dot{x}$, and $\dot{y}$ are zero. For these conditions the volume removal rate $Z = v_0 s_0$. However, when relatively compliant robots are exposed to large unpredictable forces at the tip of the arm, large deflections result and the conventional formulation is not sufficient.

In fact, even for conventional grinding when chatter occurs the deflections and velocity variations are not zero. Tobias [4] has stated that the feed velocity varies between $(v_0 - \dot{x}_{min})$ and $(v_0 + \dot{x}_{max})$ in grinding and that this phenomenon is similar to type B chatter in lathes. Consequently, the velocity v_0 in the equation for Z must be adjusted accordingly. Furthermore, the actual depth of cut is no longer equal to the desired depth of cut and s_0 must be replaced by $(s_0 - y)$ [31]. Thus, the volume removal rate in the tangential direction is now

$$Z = (v_0 - \dot{x})(s_0 - y) \tag{3}$$

In addition, if the wheel is moving in the negative y direction, material is removed in the normal direction as in plunge grinding [50]. The velocity in this direction is $-\dot{y}$, and the depth of cut can be approximated as $\lambda(s_0 - y)$, where λ is a constant derived from the process geometry. Now the total grinding forces are

$$\begin{aligned} F_n &= C_t(v_0 - \dot{x})(s_0 - y) - C_n(s_0 - y)\dot{y} \\ F_t &= \mu F_n \end{aligned} \tag{4}$$

where C_t and C_n are the proportionality constants in the tangential and normal directions respectively.

The instantaneous normal force observed in the actual experiments includes high frequency random vibrations resulting from microscopic interactions between

the wheel and the workpiece. The normal force in equation (4) does not include such high frequency vibrations since it was derived from macroscopic relations. However, the frequency range for these vibrations is at least an order of magnitude higher than the natural frequency of the robot. Therefore, these high frequency random vibrations are less significant in analyzing the dynamics of grinding with robots. Thus, the important behavior, caused by slow variations in the interactions between the wheel motion and the cutting process, is represented in equation (4) and this representation of the grinding force can be used to simulate grinding with robots.

It is clear from equation (4) that the the behavior of the grinding force is highly nonlinear. In the above development, it was implicitly assumed that the grinding wheel is always in direct contact with the workpiece surface. However, if the grinding wheel leaves the surface, additional nonlinearities must be introduced. For example, if $y > s_0$ the wheel is no longer in contact with the workpiece and $C_t = C_n = 0$. In addition, if $\dot{y} > 0$ the wheel is moving away from the workpiece and no material is removed in the y direction; therfore, under these conditions $C_n = 0$. Similarly, if $\dot{x} > v_0$ no material is removed in the x direction and $C_t = 0$.

Thus, the resulting grinding force representation and, consequently, the dynamic behavior during grinding is highly nonlinear. This is neccessary to accurately model the grinding process, because many phenomenon typically

observed in grinding experimentation, such as limit cycles with beats, can only be generated by nonlinear effects. It will be shown that the resulting equations of motion can generate nonlinear behavior similar to that observed in the experiments.

3.3 Modeling and Characterization of Tool Suspension System

The model of the tool holder structure and the grinding process geometry discussed in this research is shown in Figure 3. The x axis, in the figure, is directed tangent to the desired workpiece surface, while the y axis is normal to this surface. The origin O is coincident with the center of the wheel, when the wheel is not deflected from its desired position. As the grinding process proceeds, the Oxy coordinate frame moves at the desired feed rate v_0. The deflections of the wheel are denoted by x(t) and y(t) and they are defined, with reference to the Oxy reference frame, to be positive when directed away from the workpiece. The variations of the wheel velocity in the x and y direction from the desired velocities are represented by $\dot{x}$ and $\dot{y}$.

The grinding wheel and tool are held by a robot manipulator. The stiffness and damping of the structure in the model represent the resultant characteristics of the robot arm and the tool holder which couples the tool to the tip of the robot arm. In general, stiffness matrices of multi-axis mechanical systems have principal axes along which the stiffness is decoupled and can be

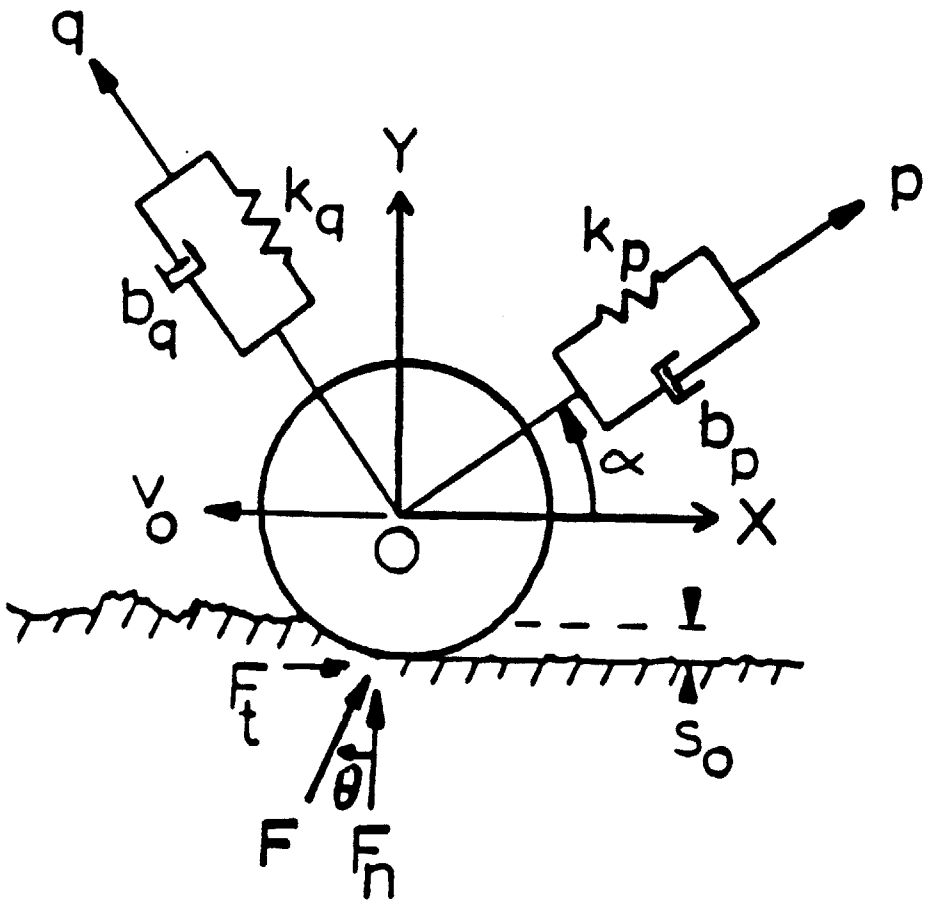

FIGURE 3: Model of Robotic Grinding Process

represented by individual springs. Although the principal axes for damping are generaly not coincident with those for stiffness this will be assumed here for simplification. Thus, as shown in Figure 3, the resultant characteristics can be represented by two springs and two dampers k_p, k_q and b_p, b_q directed along the principal directions p and q accordingly. The p and q directions are orthogonal and the origin of the Opq coordinate frame is coincident with that of the Oxy frame. The coordinates, p(t) and q(t), represent the deflections of the grinding wheel from its desired position in the p and q directions. The angle α represents the rotation of the Opq coordinate frame relative to the Oxy frame and will be referred to as the structure orientation angle. The spring constants k_p, k_q and the structure orientation angle α are the primary tool holder design parameters. These parameters are to be optimized through the investigation of their effect upon the grinding performance.

First the dynamic behavior of the tool holder is discussed. Let m be the mass of the grinding tool, then the equations of motion of the tool suspension system in the principal directions are given by

$$\begin{aligned} m\ddot{p} + b_p\dot{p} + k_p p &= f_p \\ m\ddot{q} + b_q\dot{q} + k_q q &= f_q \end{aligned} \tag{5}$$

where f_p and f_q are the components of the forces acting on the grinding wheel in the p and q directions respectively.

Surface machining processes, such as grinding, are characterized by strong coupling between the normal and tangential directions. This coupled behavior is now evaluated and an effective tool for the optimization of the design parameters is developed. As shown in Figure 3, the reaction force **F** acts upon the wheel during the grinding process. The reaction force has components in both the normal, y, and tangential, x, directions as shown in Figure 3. This relationship was discussed earlier and was presented in equation (1)

The components of the reaction force **F** in the principal directions f_p and f_q are given by

$$\begin{aligned} f_p &= F\sin(\alpha + \theta) \\ f_q &= F\cos(\alpha + \theta) \end{aligned} \tag{6}$$

Substituting equation (6) into equation (5), eliminating the force **F** and taking the laplace transform yields the following relation between the behavior along the two principal directions.

$$q(s) = \cot(\alpha + \theta) \quad \frac{ms^2 + b_p s + k_p}{ms^2 + b_q s + k_q} \quad p(s) \tag{7}$$

The final dimensions of the workpiece are directly determined by the behavior of the grinding wheel in the y direction. Deflections in the x direction, on the other hand, have no direct effect on these dimensions. Thus,

the behavior of the wheel in the y direction is of primary concern. The following coordinate transformations are now introduced.

$$\begin{aligned} x &= p\cos\alpha - q\sin\alpha \\ y &= p\sin\alpha + q\cos\alpha \end{aligned} \tag{8}$$

The resulting equation is

$$y(s) = G(s)x(s) \tag{9}$$

$$G(s) = \cot\theta \frac{ms^2 + B_t s + K_t}{ms^2 + B_n s + K_n}$$

where B_n, K_n and B_t, K_t are each a different function of α, k_p, b_p, k_q, and b_q and represent the damping and stiffness properties of the suspension system in the normal and tangential directions.

The transfer function G(s) in equation (9) represents the effect of behavior in the x direction on behavior in the y direction. This accounts for the coupling caused by the relation described in equation (1). Hanh [52] has stated that vibrations are more likely in the tangential direction than the normal direction because of relatively low process stiffness in that direction, and Tobias [13] added that vibrations in the tangential, x, direction cause pulsating normal forces, F_n. Thus, it is desirable to have the coupling as small as

possible so that deflections in the x direction have the smallest effect on the behavior in the y direction.

If only high frequency vibrations are considered the ms^2 terms in the transfer function dominate and G(s) reduces to $\cot\theta$. However, for low frequency vibrations the stiffness terms dominate in equation (9). Then the transfer function G(s) reduces to

$$G(0) = \kappa = \frac{K_t}{K_n} \cot\theta$$

$$\kappa = \frac{(d + 2)\cos\theta - d\cos(\theta + 2\alpha)}{(d + 2)\sin\theta + d\sin(\theta + 2\alpha)} \tag{10}$$

where

$$d = \frac{k_q - k_p}{k_p} > -1 \tag{11}$$

and κ represents the correlation between the behavior in the normal and tangential directions. Thus, the design parameters α, k_q, and k_p effect the coupling for low frequency vibrations. The effect of α and d on κ is shown in Figure 4 for force angles of 45 and 30 degrees.

When the value of κ is near 1, the deflections in the normal and tangential directions are approximately equal and the behavior in the two directions is strongly correlated. This strong correlation occurs when the p or the q axis is

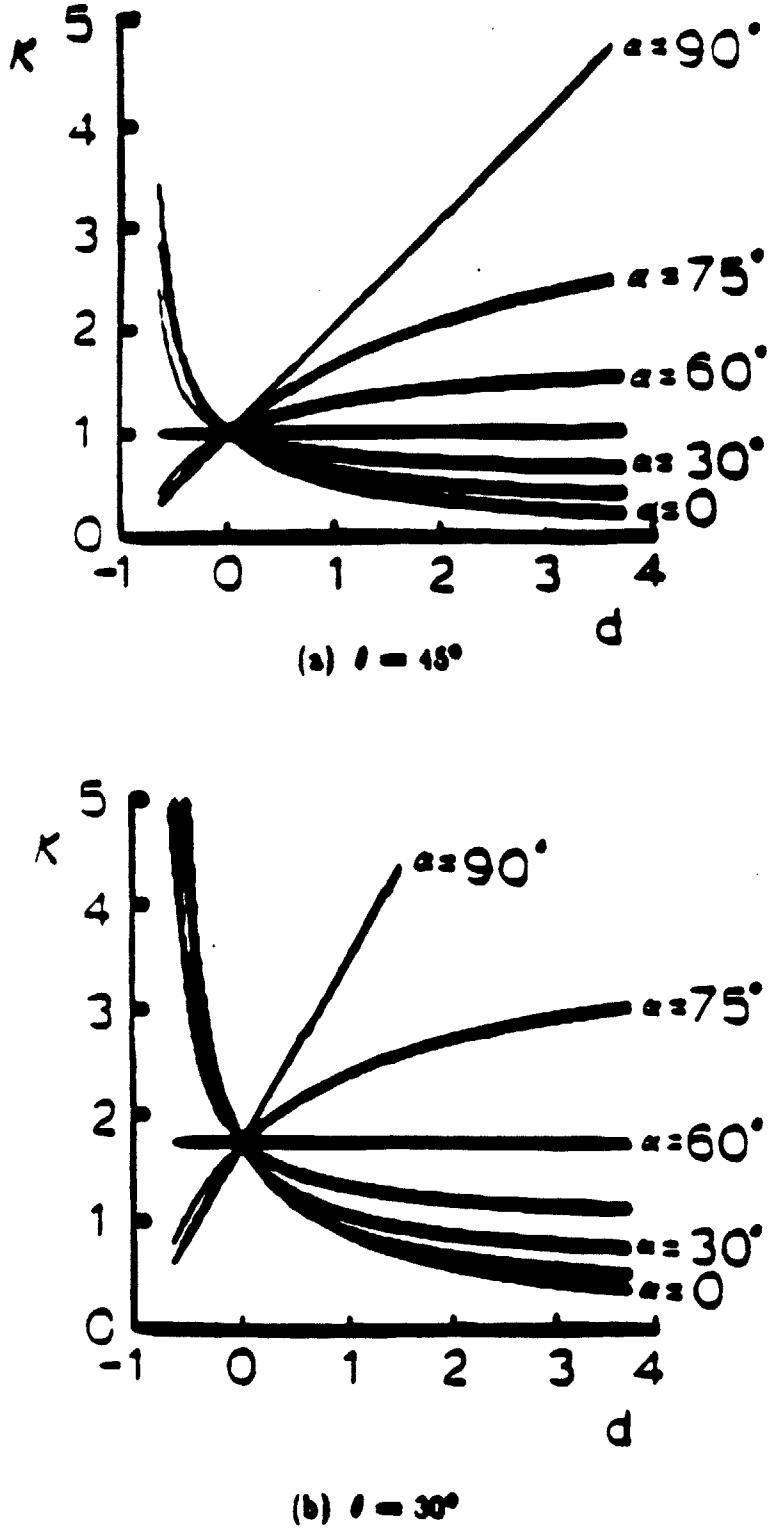

FIGURE 4: Effect of design parameters α and d on κ

directly aligned with the direction of the grinding force or when the two spring constants k_p and k_q are approximately equal. The value of κ is small when the structure orientation angle α is close to 0 degrees and d is large, or when α is close to 90 degrees and d is small. Both sets of conditions describe the same configuration for the springs which requires $K_t << K_n$. Also the value of κ is large, when $\alpha = 0$ and d is small, or when $\alpha = 90$ and d is large, namely when $K_t >> K_n$. In both cases, $\kappa << 1$ and $\kappa >> 1$, the two directions are weakly correlated. In the following chapter, it is shown that vibrations during the grinding process become large when the two axes are strongly correlated, κ near 1, and that the vibrations are significantly reduced for suspension designs which result in weak correlation, κ close to zero or infinity.

4 SIMULATION OF GRINDING WITH ROBOTS

4.1 Performance Measurement

The equations developed in the previous section are now simulated and the conclusions of the simulations are verified experimentally, in chapter 5. The objective of the simulations and the experimentation is to determine the optimal combination of directional stiffness properties and structure orientation angle.

In the simulations, external disturbances are considered by changing the initial conditions. The initial deflections are x_0 in the x direction and y_0 in the y direction. Figure 5 shows a typical simulated responce to deflections under normal grinding conditions.

In Figure 5a, $x_0 = 10$ mills and $y_0 = 0$. As mentioned before, the surface finish and the final workpiece dimensions are determined directly by the dynamic behavior of the wheel in the y direction. In order to evaluate the effect of the vibratory behavior upon the workpiece, two representative measures of performance are introduced. The maximum peak amplitude in the y direction, Y_{max} in the figure, will be used as a measure of the grinding performance in response to deflections in the x direction. The maximum peak amplitude Y_{max} can be normalized by x_0 to obtain a dimensionless performance measurement.

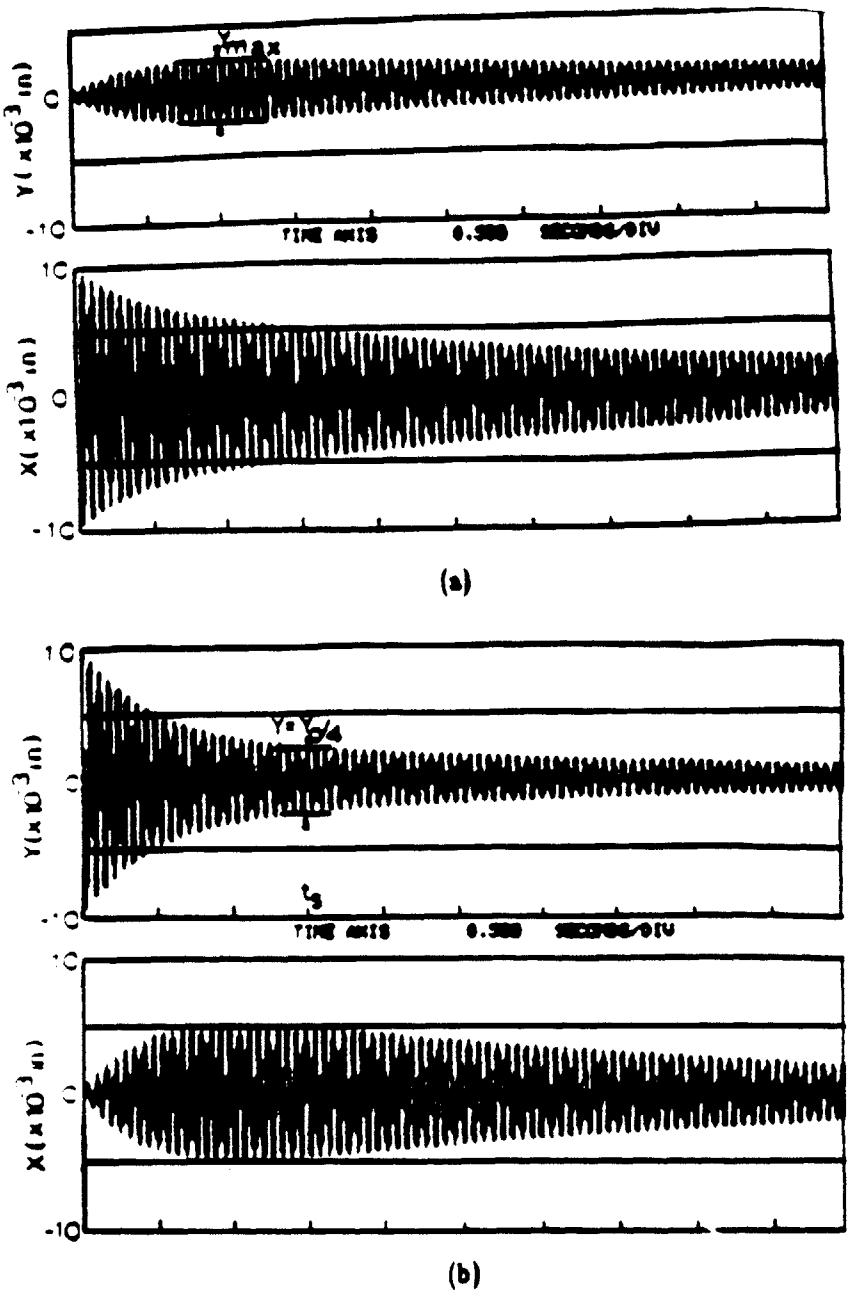

FIGURE 5: Definition of (a) Y_{max} for $y_0 = 0$, $x_0 > 0$ and (b) t_s for $0 < y_0 < s_0$, $x_0 = 0$.

For deflections in the y direction, the behavior is shown in Figure 5b for the same design parameters. In this case, the time, t_s, required to reduce the vibration amplitude to $y_0/4$ is used as a measure of performance.

4.2 Worst Case

The worst grinding performance was observed in the simulations when $k_p=k_q$ and $b_p=b_q=0$; this corresponds to a correlation of 1. Under these conditions, if the wheel is deflected in either the x or the y direction the result is a large stable limit cycle, as shown in Figure 6. In order to illustrate the dynamic responses for a long time period, phase plane plots are used. Both the x and y responses become stable limit cycles in the steady state.

When damping greater than zero is introduced with the same conditions as in Figure 6 the behavior shown in Figure 5 results.

4.3 Effect of Correlation on Grinding Performance

Figures 7 and 8 summarize the effects of the correlation factor κ on the grinding performance with α set to zero. Clearly, the worst behavior is observed when $K_t=K_n$. Thus, the best disturbance rejection is obtained when the stiffness in the principal directions are far apart.

From Figures 7 and 8 it appears that either high or low values of κ will provide good performance. High values of κ occur when $K_n<<K_t$ and low

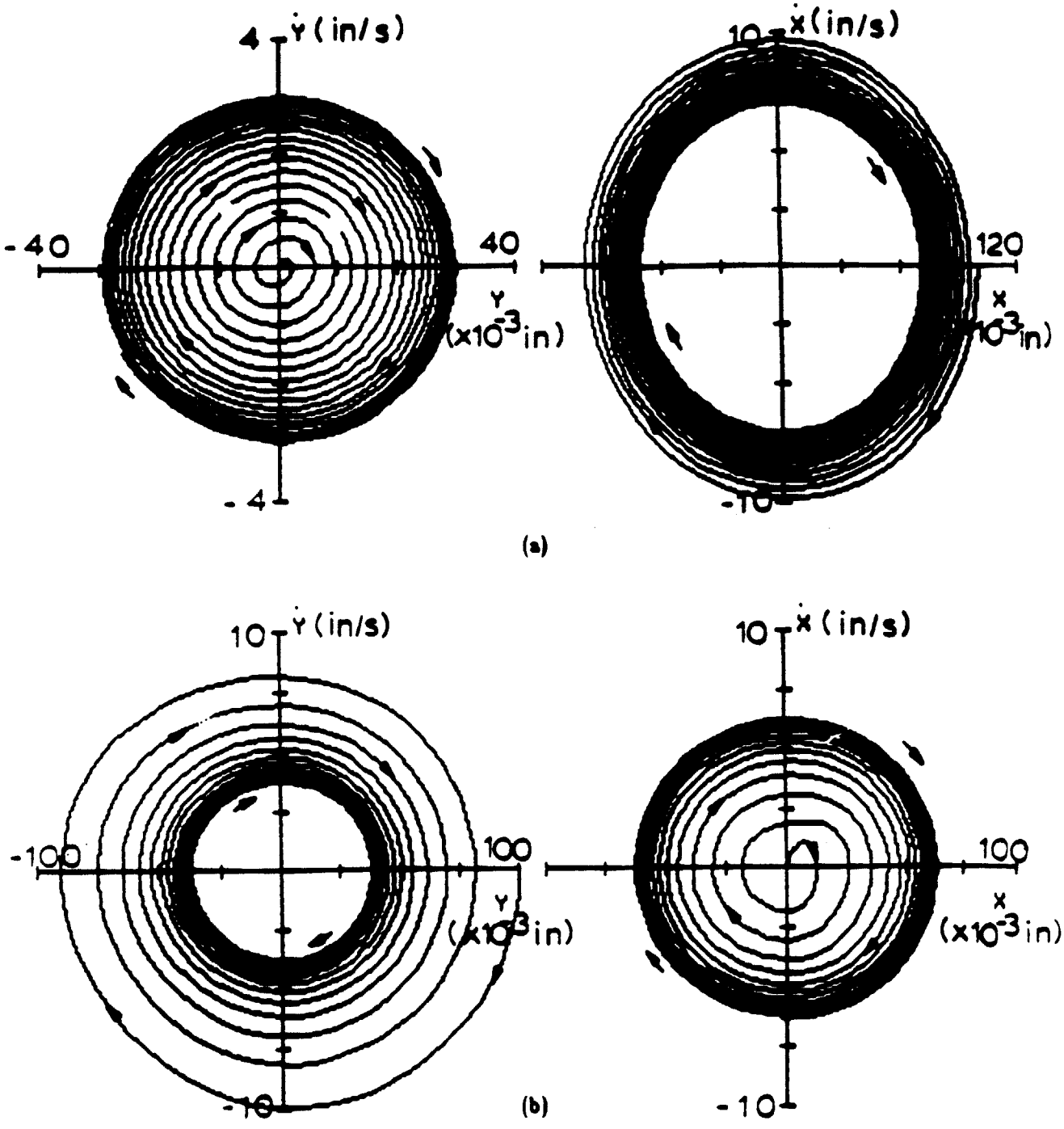

FIGURE 6: Simulated phase plane plots for (a) $x_0 = 0.1$ in, $y_0 = 0$ and (b) $x_0 = 0$, $y_0 = 0.1$ in.

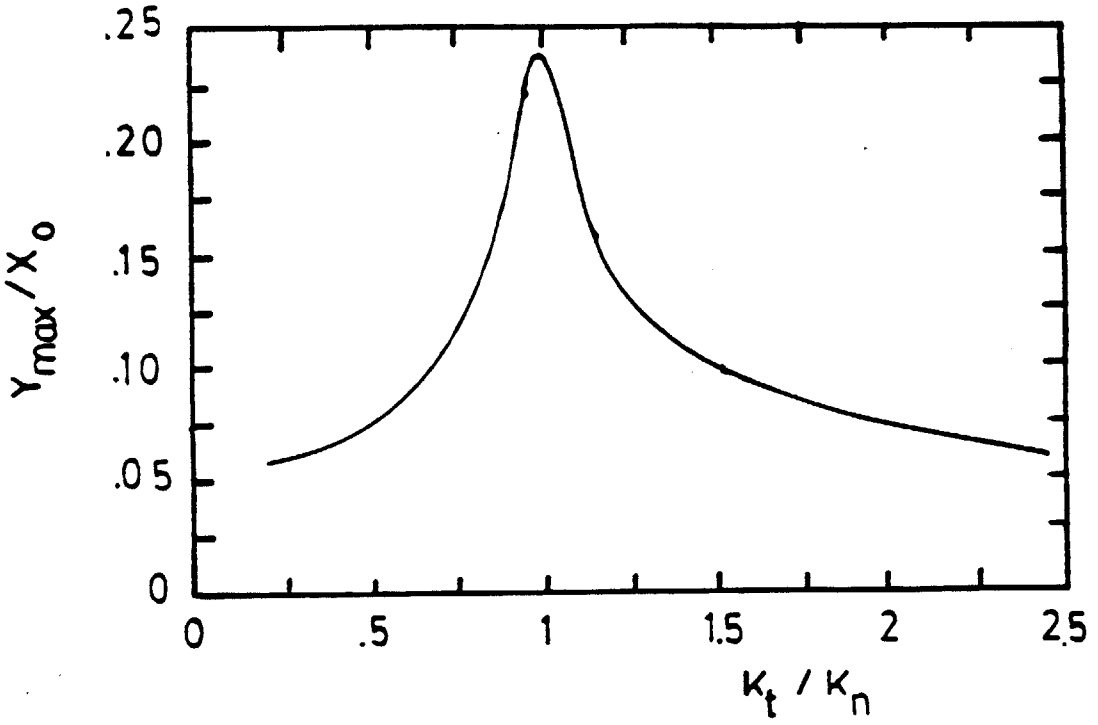

FIGURE 7: Simulated effect of directional stiffness properties K_t/K_n ($= \cot\theta/\kappa$) on Y_{max}/x_0 for $y_0 = 0$, $x_0 > 0$

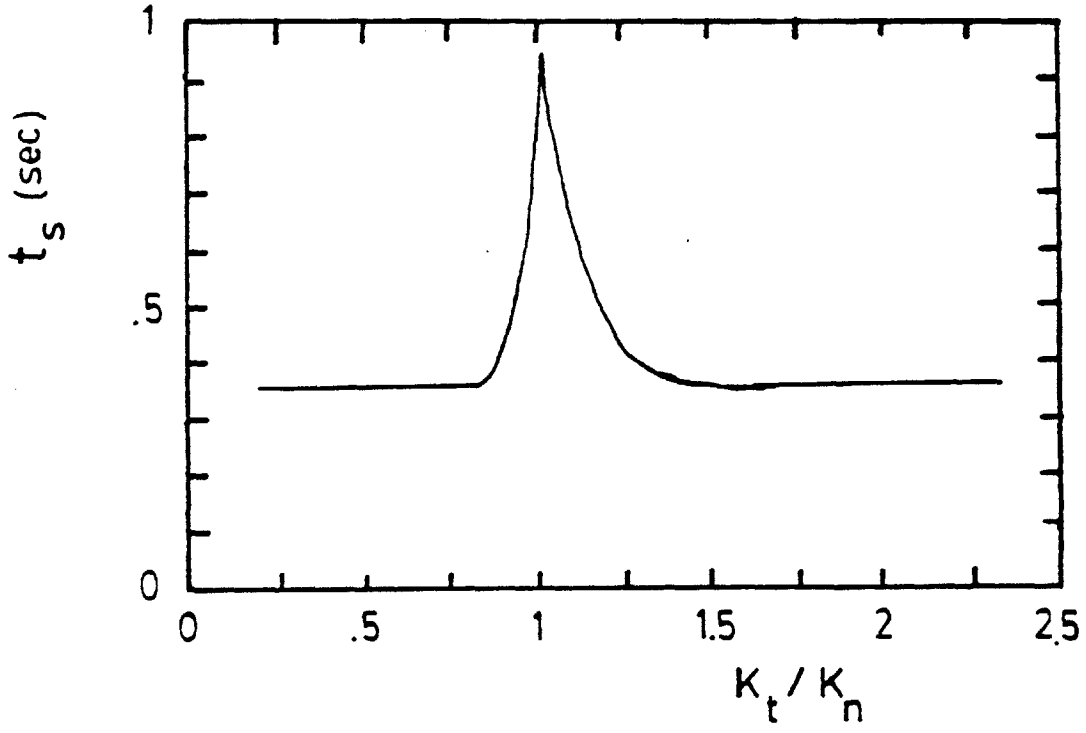

FIGURE 8: Simulated effect of directional stiffness properties K_t/K_n ($= \cot\theta/\kappa$) on t_s for $0 < y_0 < s_0$, $x_0 = 0$

values of κ occur when $K_t << K_n$. However, the maximum stiffness attainable is limited by the maximum stiffness of the robot arm. From the complete equations of motion it can be found that the steady state deflection in the y direction, Y_{ss}, is directly related to the stiffness in the normal direction by

$$Y_{ss} = \frac{C_t v_0 s_0}{K_n + C_t v_0} \tag{12}$$

This steady state deflection limits the attainable accuracy of the process. Since Y_{ss} decreases as K_n increases, it is desirable to have K_n as large as possible and the robot should be oriented with its largest stiffness in the normal direction. Since the maximum stiffness is now in the normal direction good grinding performance is only possible when $K_t << K_n$.

4.4 Effect of Structure Orientation Angle

Clearly, the condition when $k_q = k_p$ must be avoided and $k_p << k_q$ is desirable. However, the optimal orientation angle when $k_p << k_q$ must still be determined. The simulation results for $x_0 = 5$ mills and $k_p << k_q$ are shown in Figure 9.

In this case, the force angle was set to 30 degrees to emulate conditions observed in experiments and to permit comparison. The worst behavior is now observed when α equals 45 or -45 degrees. The best behavior occurs when α equals zero.

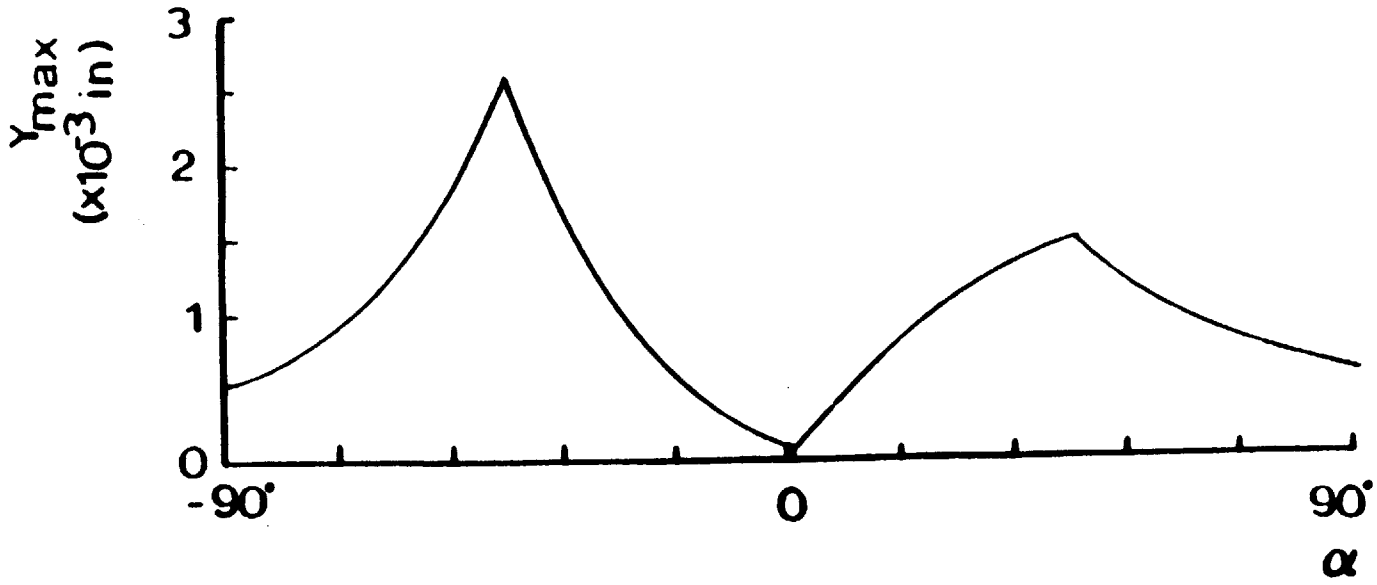

FIGURE 9: Simulated effect of α on Y_{max} for $x_0 = 5x10^{-3}$ in and $y_0 = 0$

In the following section it will be shown that the behavior generated in the simulations is similar to that observed in the experimentation. In addition, the conclusions of the simulations for the effect of the structure orientation angle on grinding performance will be confirmed experimentally.

5 GRINDING EXPERIMENTATION

5.1 Experimental Setup and Procedure

Each experiment discussed in this section was run with a 6 inch diameter, 1 inch thick, hard cylindrical grinding wheel, a 2.5 Hp grinding tool rotating at 1200 rmp, a 20 x 10^{-3} inch desired depth of cut, a 0.33 inch/sec feed rate and a 2 inch long preground mild steel workpiece.

A compliant wrist was designed to permit the variation of the tool holder's directional stiffness properties. The wrist was also equiped with strain gages for force measurement, and the experimental data was sampled at 500Hz by a Digital PDP/11 computer. Pictures of the experimental setup. are provided in Figure 10.

5.2 Comparison of Experimental and Simulated Behavior

The validity of the model is verified by comparing the simulation output with the behavior observed in experiments for similar conditions. Figure 11a shows the results of an experiment in which α = -45 degrees and $k_q = 10k_p$. The higher frequency vibration in the experiment is about 20Hz, which is the same as that of the wheel rotation, and is caused by wheel imbalance. This situation is simulated by introducing a disturbance in the workpiece surface of 1 mill amplitude and 20Hz frequency. The results of the simulation are shown

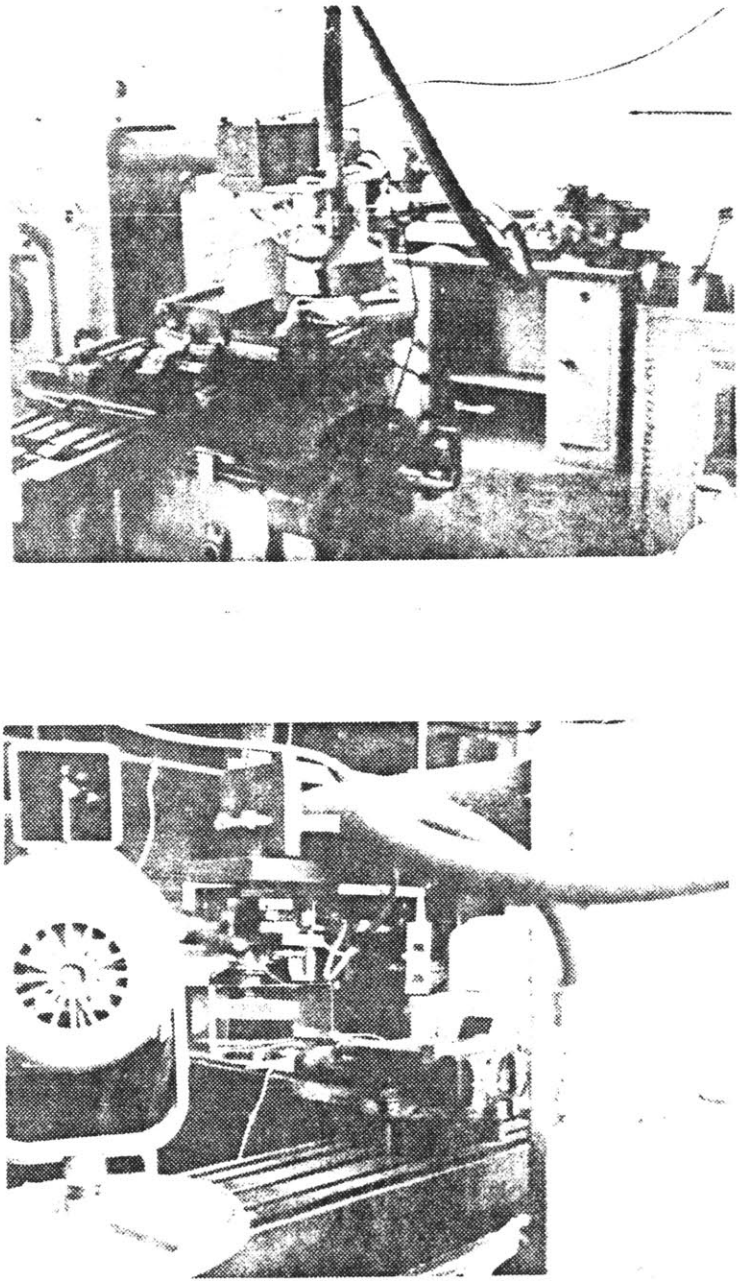

FIGURE 10. Photographs of experimental setup

in Figure 11b for the same directional stiffness properties and orientation angle as in the experiment. In each case, a similar beating phenomenon is observed at roughly the same frequency and amplitude. Thus, the model can generate similar behavior to that observed in the experimentation.

To verify the conclusions of the simulations the optimal orientation angle was also determined experimentally. A schematic of the wheel and workpiece orientation for the experiments is shown in Figure 12a.

The actual force data for these experiments is shown in Figures 12b through 12e for α = -45, 0, 45, and 90 degrees. From the force data in Figures 12b and 12d it is clear that orientation angles of 45 and -45 degrees produce highly erratic behavior during grinding. When $\alpha = -45^{o}$ the high stiffness direction is aligned with the resultant grinding force and the behavior appears to be a high frequency limit cycle with low frequency beats. This phenomenon is comon in grinding practice and it was found that the number of beats observed in the force data showed up directly on the workpiece surface as an equivalent number of undesirable low frequency waves. When $\alpha = 45^{o}$ the low stiffness direction is aligned with the resultant grinding force and the deflections are large and erratic; this appears to be the worst tool holder compliance design. In Figures 12c and 12e it appears that orientation angles of 0 and 90 degrees both result in relatively stable grinding. For each of these

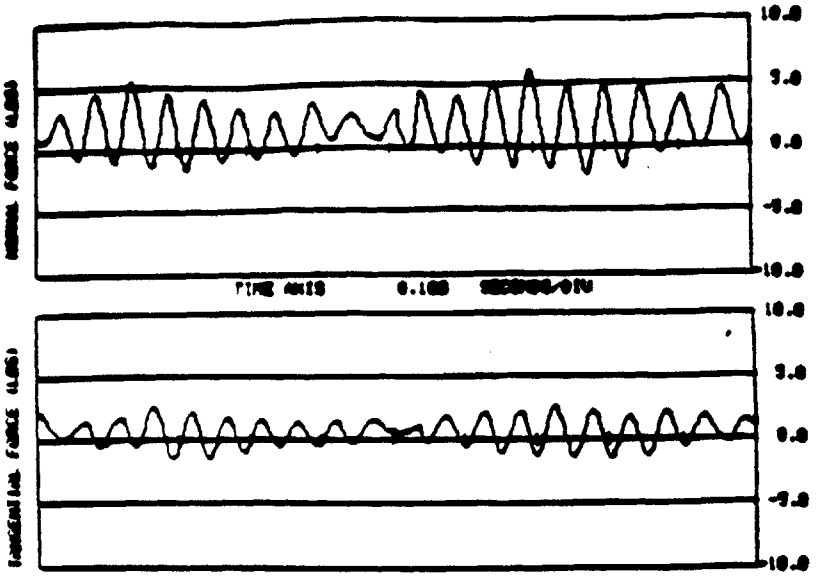

(a)

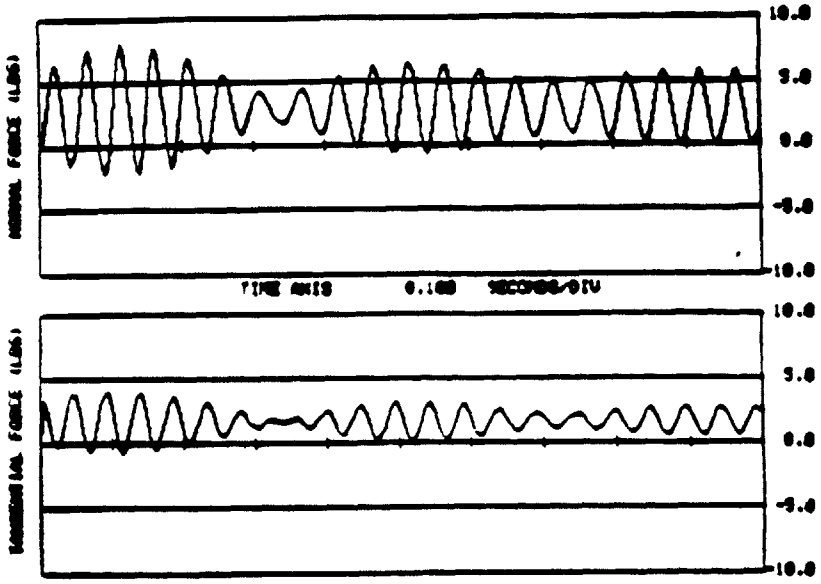

(b)

FIGURE 11: Comparison of (a) experimental and (b) simulated grinding data for $\alpha = -45^{\circ}$ and $k_q = 10k_p$.

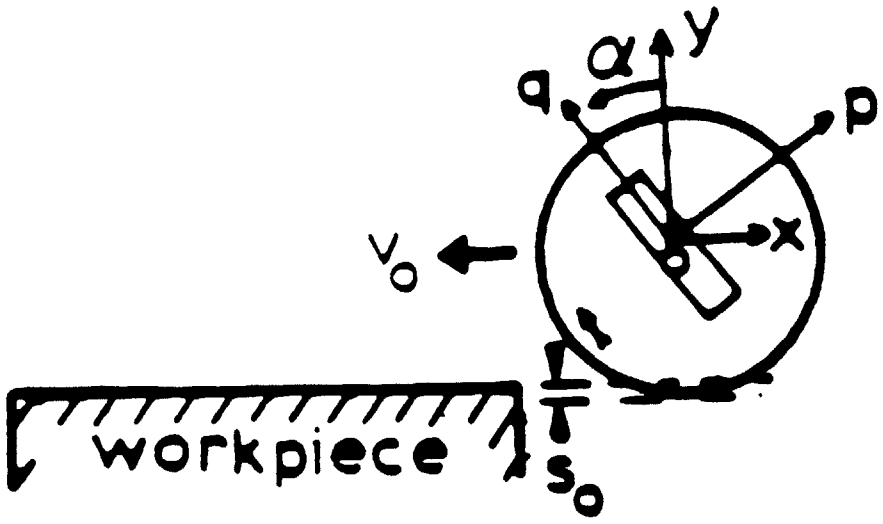

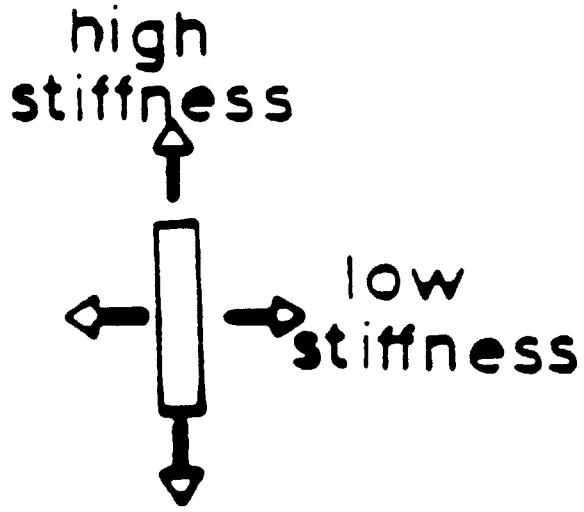

FIGURE 12a: wheel/workpiece orientation for grinding experiments

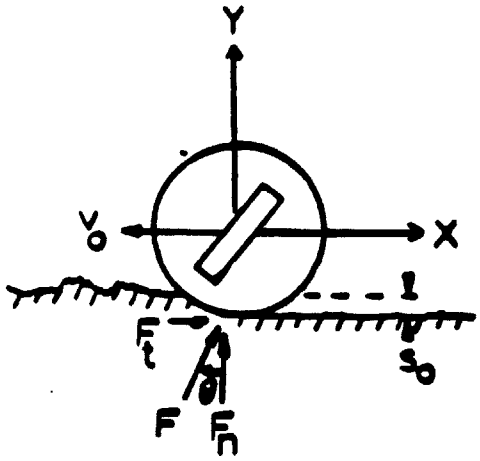

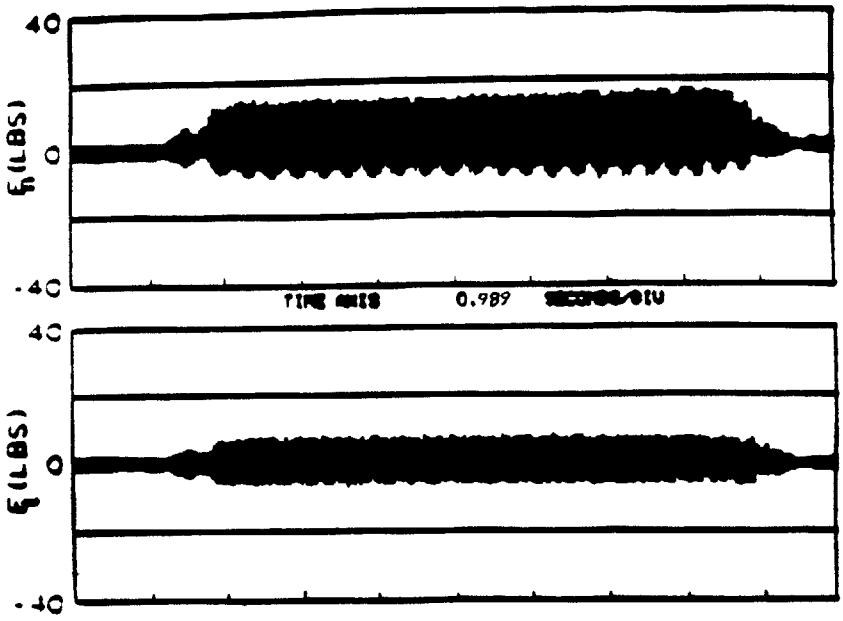

FIGURE 12b: Experimental grinding data for $k_q=10k_p$ and $\alpha=-45^\circ$

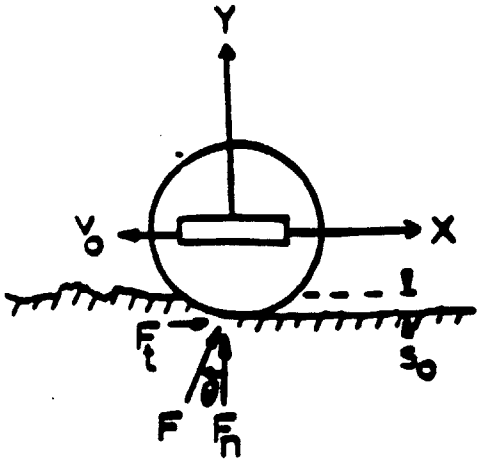

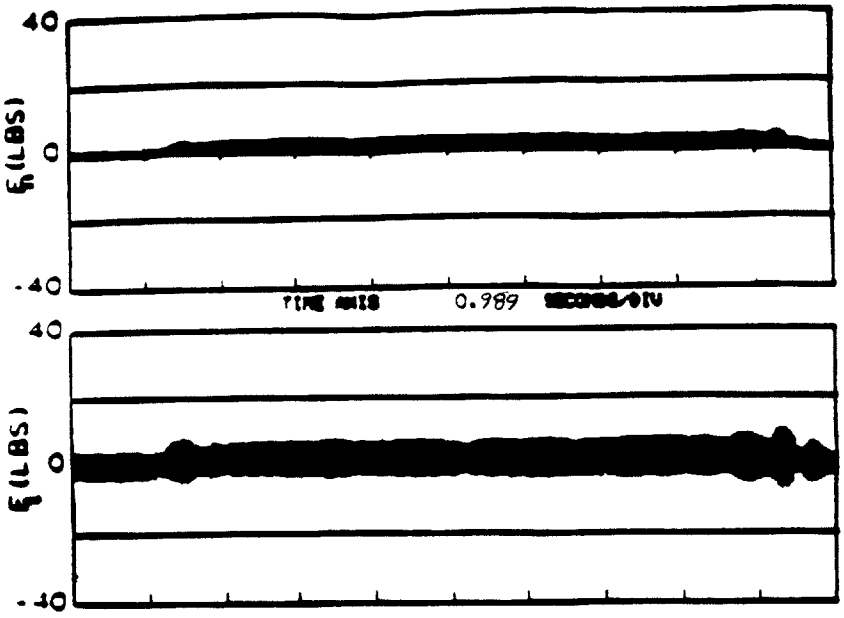

FIGURE 12c: Experimental grinding data for $k_q=10k_p$ and $\alpha=0$

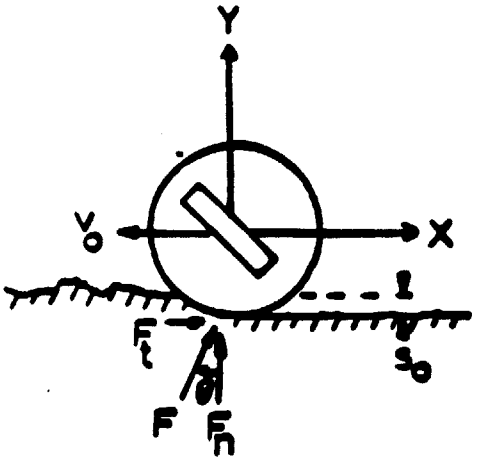

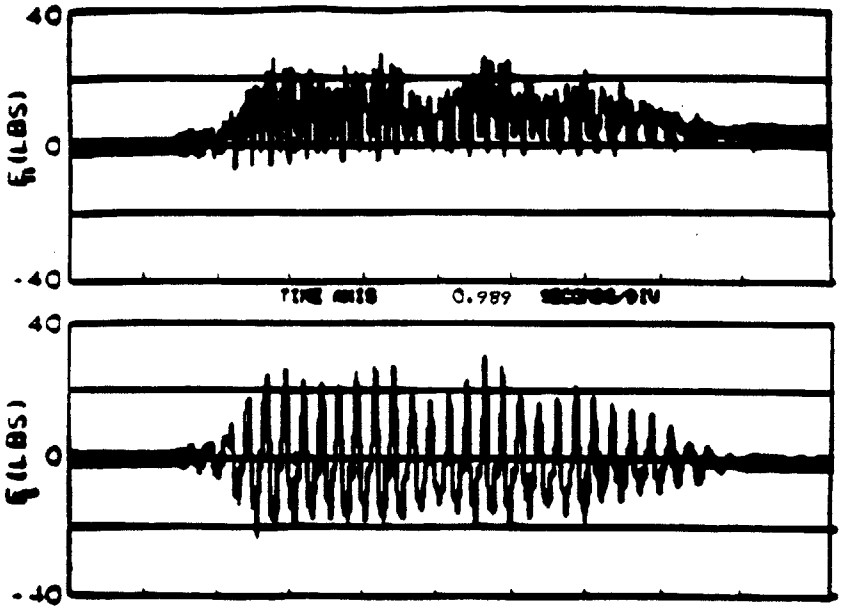

FIGURE 12d: Experimental grinding data for $k_q=10k_p$ and $\alpha=$ 45°

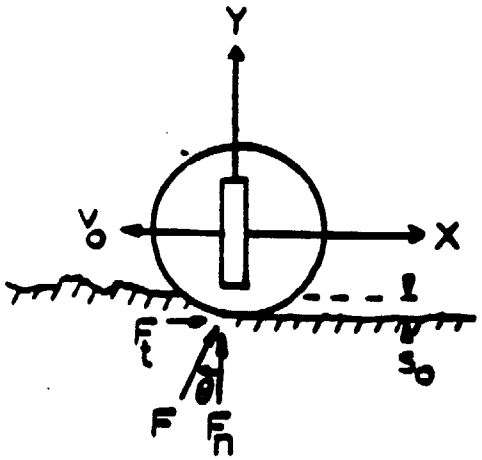

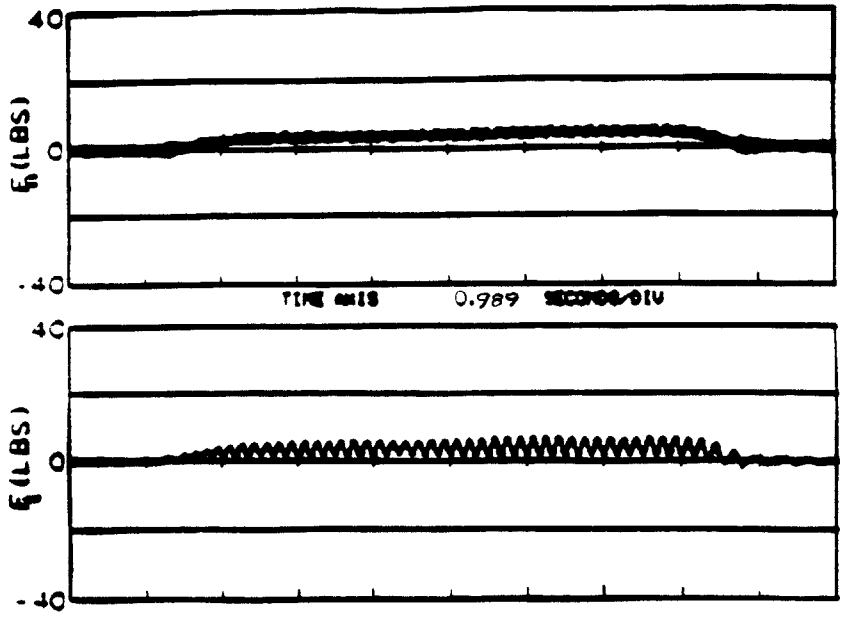

FIGURE 12e: Experimental grinding data for $k_q=10k_p$ and $\alpha=$ 90°

tool holder designs it was found that an excellent surface finish could be obtained. To determine which of these designs provides the best overall grinding performance it is neccessary to consider the magnitude of the deflections as well as the degree of stability in the grinding forces.

The maximum deflections for each of the experiments are shown in Figure 13 in the same form as the simulated data in Figure 11 to permit comparison, except in the experiments the disturbances are unknown and the maximum deflection Y_{max} is not normalized. In addition to the maximum deflection in the y direction, the average deflection is also plotted in Figure 13 to provide a measure of the actual depth of cut. When $\alpha = 90^{o}$ and $k_p << k_q$ the stiffness in the normal direction is low and consequently, the average deflection, Y_{avg}, caused by the grinding force is relatively large. This results in very low material removal rates and very poor accuracy, since Y_{avg} represents the average difference between the actual and desired depth of cut.

The best overall behavior is observed in the experiments when $\alpha = 0$ and $k_p << k_q$. Under these conditions $K_n >> K_t$ and the average deflection and the maximum vibration amplitudes are both minimum, as shown in Figure 13. Thus, for these conditions the accuracy, stability, and material removal rate are optimal.

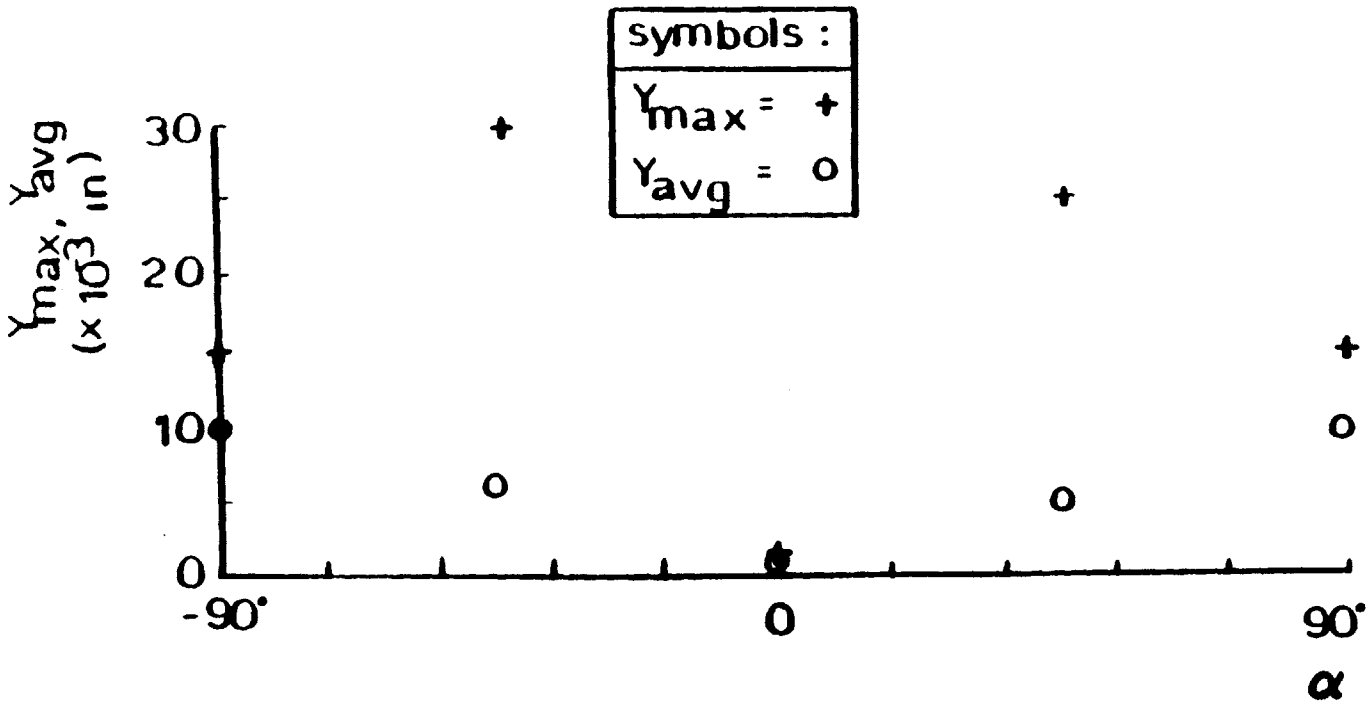

FIGURE 13: Experimental effect of α on Y_{max} and Y_{avg} for $x_0 = 5x10^{-3}$ in and $y_0 = 0$

These design conclusions are extremely important in robotic grinding for several reasons:

1. Existing robots are characterized by large variation in directional stiffness properties. For example a SCARA type robot may appear much stiffer in the vertical direction than in the horizontal direction. Thus, the design conclusions can be utilized to improve the design of the main robot, as well as to determine which configuration of the robot will provide the best grinding performance.

2. It may be possible to improve the stiffness of an existing robot in only one direction without significantly reducing the workspace or mobility. The design conclusion state in which direction high stiffness is most important.

3. Many investigators have attempted to introduce additional compliance or "elastic suspension" to reduce chatter, but no complete justification for the orientation of this compliance, with respect to the workpiece surface, has been provided. The design conclusions state clearly in which direction this compliance should be located.

6 END-EFFECTOR DESIGN AND IMPLEMENTATION

6.1 Design Objectives

The design conclusions reached in the analysis and expermentation are now incorporated into a practical grinding end-effector. The designs for two grinding end-effectors, which have been constructed and tested are also briefly discussed. The major design goal is to improve the dynamic behavior during grinding by optimizing the end-effector mechanical design. Some important design issues and objectives are

1. It is desirable to maintain the highest stiffness possible in the normal direction. Therefore, the end-effector and the main robot orientation which provides the highest stiffness normal to the workpiece must be determined.

2. It has been shown that low compliance in the tangential direction improves the grinding performance. However, there is a tradeoff between the compliance and the magnitude of deflections. Thus, the tangential compliance which provides good stability and does not require an unreasonably large linear range for the spring stroke must be determined for the given grinding conditions. This compliance is determined through simulation in section 6.2.

3. The practical implementation of the design also requires sensors to accurately locate the workpiece and to control the end-effector motion. Although control and implementation is beyond the scope of this research, some basic steps have been taken in this area to permit the testing of the design conclusions.

6.2 Determination of Tangential Compliance Characteristics

As stated in section 6.1, it is necessary to determine the required tangential spring constant and to estimate the required linear range for the spring stroke. The required linear range is determined by the magnitude of the deflections in the tangential direction during normal grinding conditions. The best method available to estimate this linear range is simulation.

As an example, if the grinding wheel is deflected in the normal direction the behavior shown in Figure 14a will result when the normal and tangential stiffness is equal (Kn = Kt). If the tangential stiffness is reduced to Kn/10 or Kn/1000 the behavior shown in Figure 14b and 14c results. As can be seen from these two figures, as the tangential stiffness is reduced the behavior in this tangential direction is approaching that of a second order critically damped system. Consequently, is is possible to obtain critically damped behavior in the tangential direction by further reducing the tangential stiffness as in Figure 14d.

From Figure 14d it is now possible to estimate the required linear range for the spring stroke. Although it may be possible to further reduce the tangential stiffness it appears that doing so will only increase the required linear range without significantly improving the grinding performance.

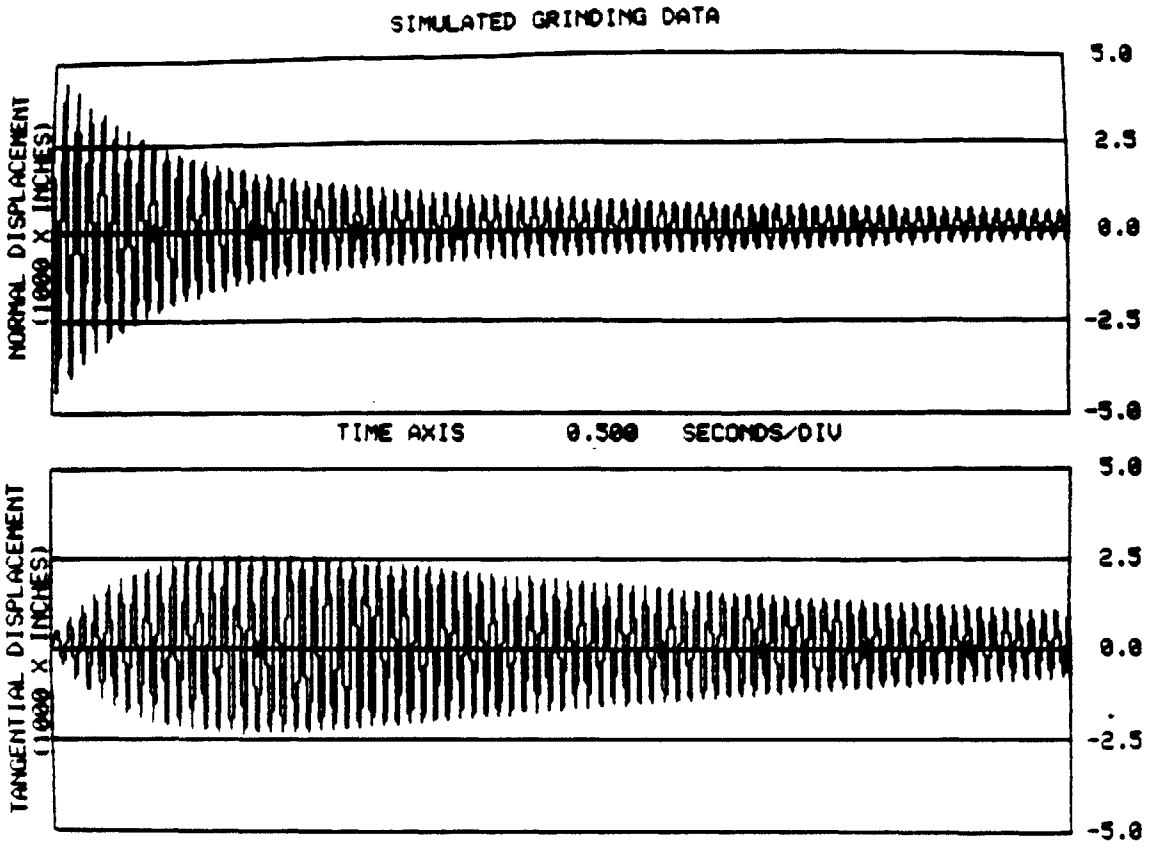

FIGURE 14a: Effect of tangential compliance on grinding behavior for $K_t = K_n$

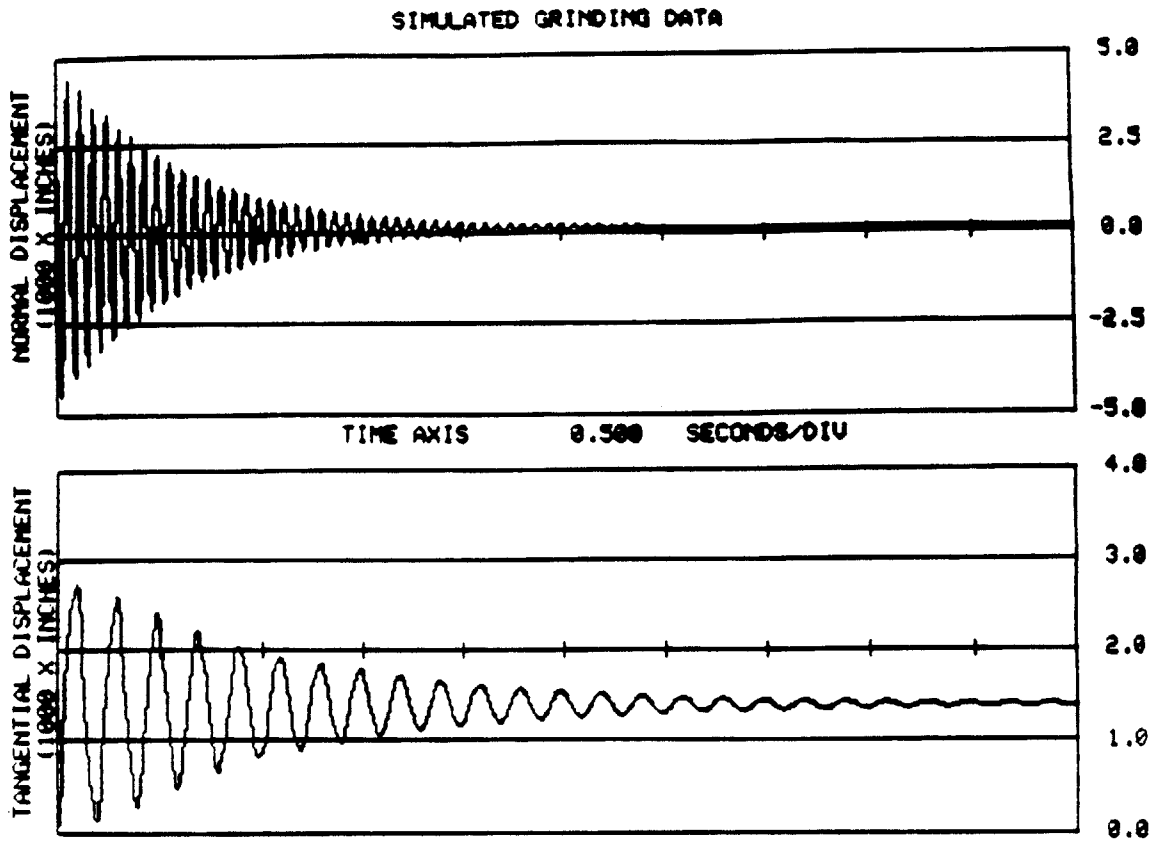

FIGURE 14b: Effect of tangential compliance on grinding behavior for $K_t = K_n/10$

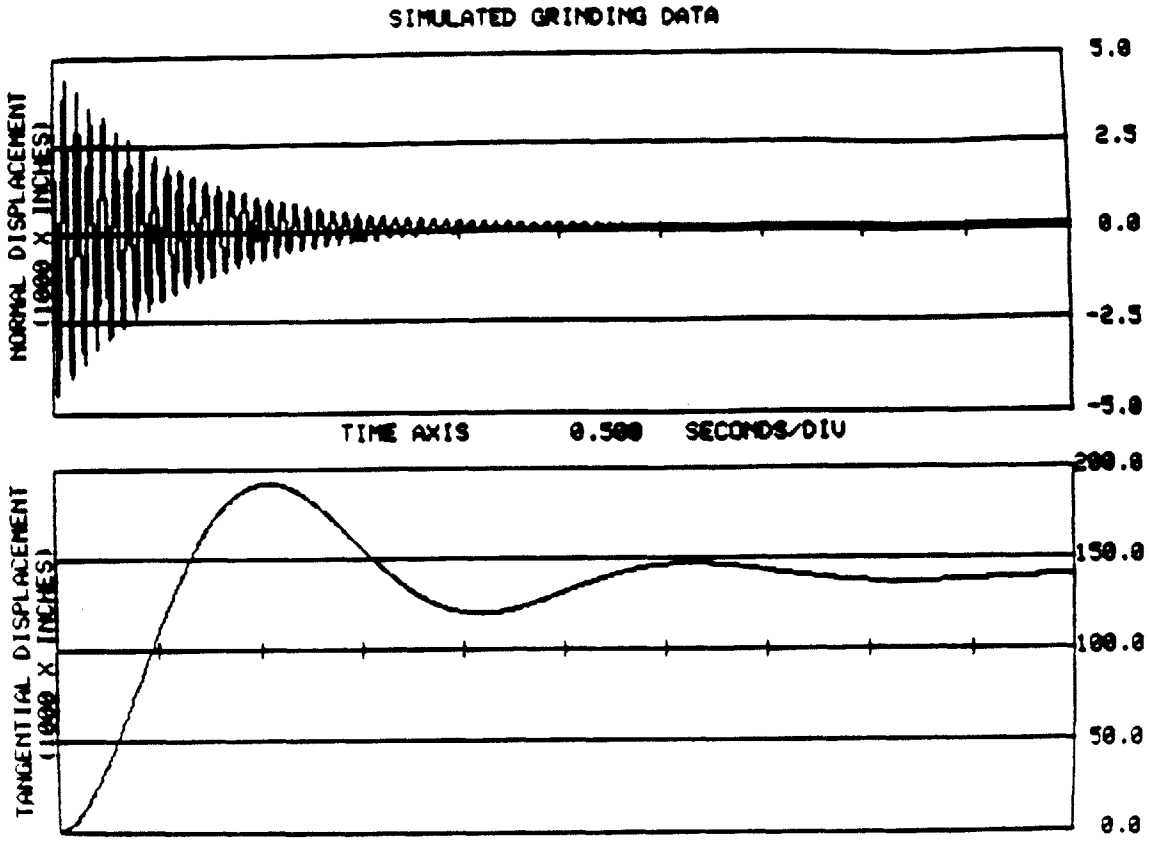

FIGURE 14c: Effect of tangential compliance on grinding behavior for $K_t = K_n/1000$

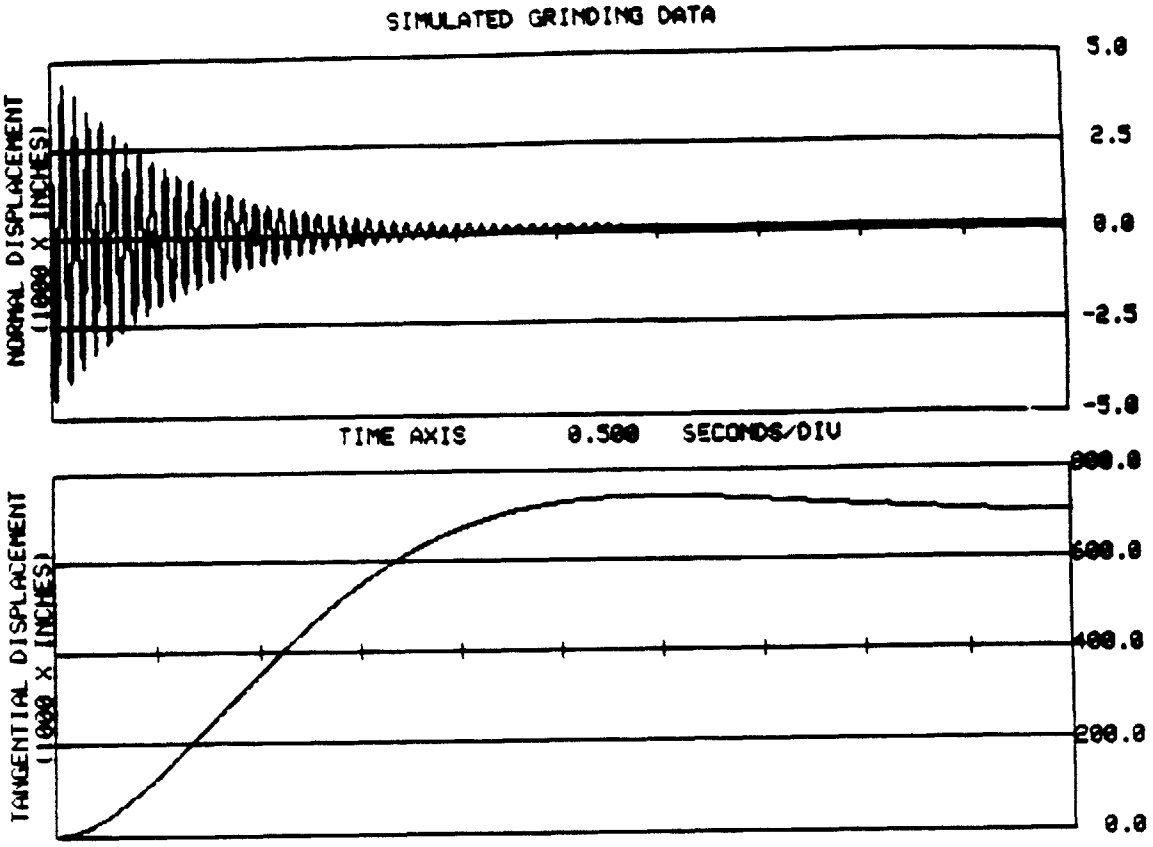

FIGURE 14d: Effect of tangential compliance on grinding behavior for $K_t = K_n/5000$

6.3 Implementation

The design conclusions have been incorporated in two grinding end-effectors. The first version is purely passive and was designed for the American Robot. This end-effector is equipped with two linear potentiometers. The first potentiometer is used to accurately locate the workpiece surface. The second potentiometer is used to measure the deflection of the spring in the tangential direction. This information also provides a rough measure of the actual depth of cut. The end-effector is equipped with a pneumatic grinding tool with a 3 inch cylindrical grinding wheel. Photographs of this end-effector are provided in Figure 15.

The second version is shown in Figure 16. This end-effector was designed for heavy duty grinding and deburring with a heavy duty robot designed and built by Daikin Industries and M.I.T.. The end-effector uses a 6 inch grinding wheel with a 2.5 hp motor. It is also equipped with a hydraulic actuator in the normal direction and a passive spring and damper in the tangential direction. This end-effector has been successfully tested on the grinding of weld seams. Over 30 mills was removed from a weld seam in a single pass with little noticable chatter and a very good surface finish.

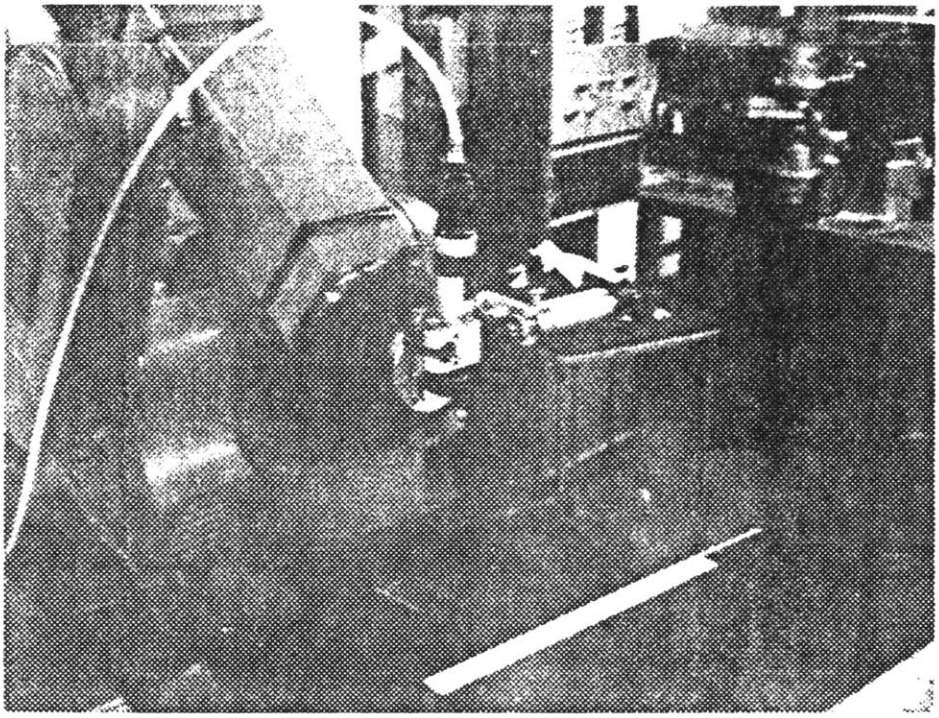

FIGURE 15a: American Robot and end-effector photograph

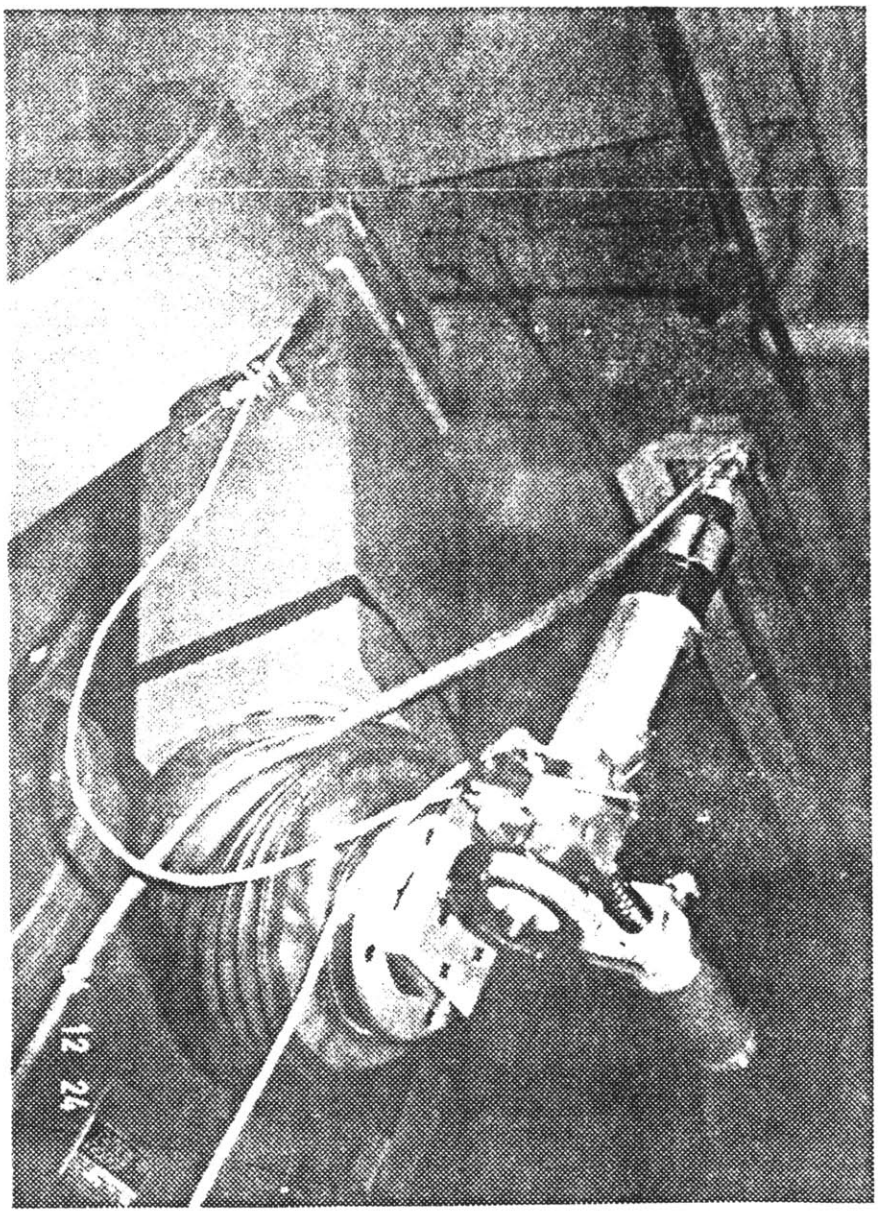

FIGURE 15b: American Robot and end-effector photograph

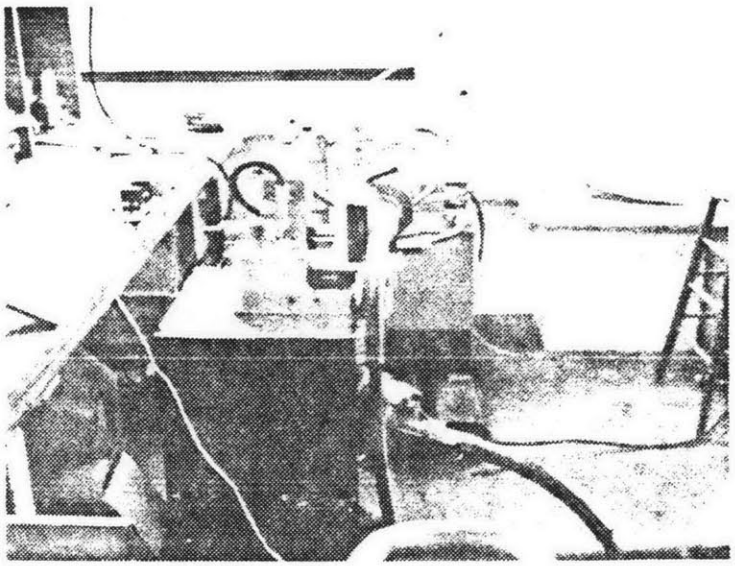

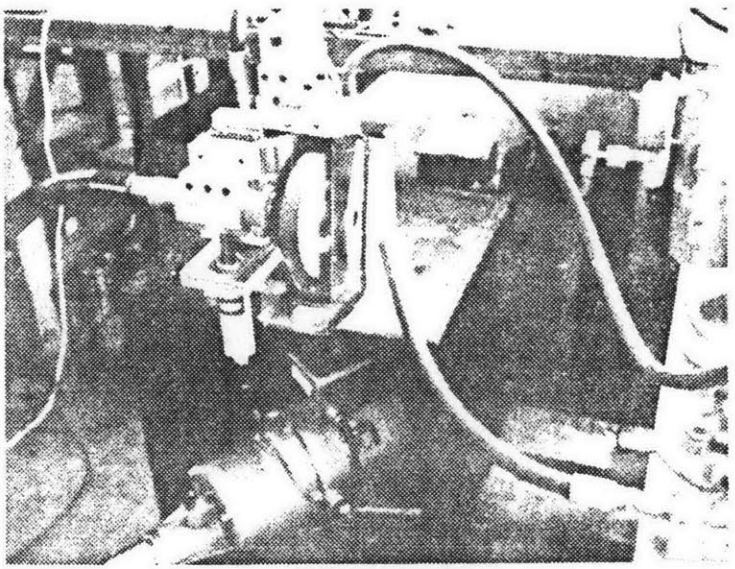

FIGURE 16: Daikin Robot and end-effector photographs

7 CONCLUSION

The optimal tool holder design for grinding with robots has been determined through dynamic analysis, simulation and experimentation. It is found that a tool holder suspension system with $k_p << k_q$ and $\alpha=0$ provides the best overall grinding performance.

Further, analysis has shown that the behavior in the tangential direction can be improved by introducing a passive damper in that direction. This is only practical because the vibrations in the tangential direction have a large amplitude and low frequency as a result of the relatively low stiffness in that direction, $K_t << K_n$.

The emphasis of this research has been process analysis and mechanical design. However, additional steps have been taken in control and implementation. For each of the end-effectors described in section 6.3 a control scheme similar to that used in "Automatic Cut Segmentation" on NC lathes [53] is being developed. In this approach the feed and depth of cut are controlled to maintain a constant cutting power. This approach has been implemented on the American Robot with some success, and further development is underway.

REFERENCES

1. Mortensen, A., "Automatic Grinding," Proceedings: 13th International Symposium on Industrial Robots, April 1983, p. 8-1 to 8-11.

2. Gustafsson, L., " Deburring with Industrial Robots," SME Deburring and Surface Conditioning Conference, 1983.

3. Plank, G. and Hertzinger, G., " Controlling a Robot's Motion Speed by a Force-Torque-Sensor for Deburring Problems," Institut fur Dynamik der Flugsysteme, D-8031 Wessling/obb. W-Germany.

4. Tobias, S. A., Machine Tool Vibrations, Authorized translation by Burton, A. H., John Wiley & Sons, Inc., New York, 1965.

5. Kuntze, H. B., " On the Closed-Loop Control of an Elastic Industrial Robot,"Proceedings: 1984 American Control Conference, June 1984.

6. Paul, F. W., Gettys, T. K. and Thomas, J. D., " Definning of Iron Castings Using a Robot Positioned Chipper," Proceedings: Robotics Research and Advanced Applications, ASME, 1982, p. 269-278.

7. Sharon A. and Hardt D. E., " Enhancement of Robot Accuracy Using Endpoint Feedback and a Macro-Micro Manipulator System," Proceedings: 1984 American Control Conference, June 1984, p. 1836.

8. Asada, H. and West, H., "Kinematic Analysis and Design of Tool Guide Mechanisms for Grinding Robots," Proceedings: Computer-Integrated Manufacturing and Robotics, New Orleans, December 1984.

9. Asada, H. and Sawada, Y., "Design of an Adaptable Tool Guide for Grinding Robots," ASME Design Engineering Technical Conference paper No. 84-DET-41.

10. Moore, S. R. and Hogan, N., "Part Referenced Manipulation-A Strategy Applied in Robotic Drilling," Control of Manufacturing Processes and Robotic Systems, ed. Hardt, D., Nov. 1983, p. 183-198.

11. Shaw, M., Metal Cutting Principals, 3rd Edition, M.I.T. Cambridge, Massachussetts, 1954. p. 18-1.

12. Doi, S., "An Experimental Study in Chatter Vibration in Grinding Operations." Trans. ASME, N0. 1, 1958.

13. Hahn, R., " On the nature of the grinding process," Proc. 3rd M.T.D.R. Conf., Pergamon Press, Oxford, p.129.

14. Konig, W. and Steffens, " A Numerical Method to Describe the Kinematics of Grinding," Annals of the CIRP, Vol ,31/1, 1982. p. 201.

15. Lindsay, R., "A Comparison of Cutting and Grinding Data," NAMRC X, SME, Dearborn, Michigan. 1982.

16. Peters, J., " The Proper Selection of Grinding Condintions in Cylindrical Plunge Grinding," Proceedings of the 16th International M.T.D.R. Conf., MacMillan Press Ltd., Publishers.

17. Koenigsberger,D., Tlusty, J., Machine Tool Structures, chapter 6 "Grinding" by M. Polecek, Pergaman press,NY, 1970, p. 331.

18. Saini, D., " Elastic Deflections in Grinding," Annals of the CIRP. Vol 29/1, 1980. p. 189.

19. Salje, E. and Dietrich, W., " Analysis of Self Excited Vibrations in External Cylindrical Plunge Grinding," Annals of the CIRP. Vol 31/1, 1982. p. 255

20. Snoeys, R. and Brown, D., " Cause and Control of Chatter Vibrations in Grinding Processes," American Society of Tool and Manufacturing Engineers, Technical Paper MR68-102.

21. Baylis, R. and Stone, J., " The Build Up and Decay of Vibrations During Grinding," Annals of the CIRP Vol 32/1,1983. p. 265.

22. Snoeys, R. and Brown, D., " Dominating Parameters in Grinding Wheel-and Workpiece Regenerative Chatter," ASME technical paper No. MR68-102.

23. Kaliszer, H., " Analysis of Chatter Vibrations During Grinding," Proc. M.T.D.R.,1970, p. 615.

24. Sexton, J. and Stone, B., " The Development of an Ultrahard Abrasive Grinding Wheel which Suppresses Chatter," Annals of the CIRP Vol 30/1, 1981.

25. Pahlitzsch, G. and Cuntze, E., "Reduction of Chatter Vibration During Cylindrical and Plunge Grinding Operation," Proc. of M.T.D.R. 1976.

26. Kumar, K. and Shaw, M., " The Role of Wheel-Work Deflection in Grinding Operations," ASME, Journal of Engineering and Industry, Feb 1981, Vol. 103, p. 73.

27. Saini, D., Wager, J. and Brown, R., "Practical Significance of Contact Deflections in Grinding," Annals of the CIRP 31/1, 1982. p. 215.

28. Nakayama, K., Brecker, J. and Shaw, M., "Grinding Wheel Elasticity," ASME, Journal of Engineering and Industry, May 1971, p. 609.

29. Hahn, R., Discussion of " Grinding Wheel Elasticity" by Nakayam, Becker and Shaw, Journal of Engineering and Industry, May 1971.

30. Hahn, R. and Price, R., "A Nondestructive Method of Measuring Local Hardness Variations in Grinding Wheels," Annals of the CIRP, Vol. 16, p. 19.

31. Snoeys, R. and Wang, I., " Analysis of the Static and Dynamic Stiffness of the Grinding Wheel Surface," Proc. M.T.D.R, 1969, p. 1133.

32. Brown, R., Saito, K. and Shaw, M., "Local Elastic Deflections in Grinding," Annals of the CIRP Vol XVIV, 1971. p.105.

33. Hahn, R. and Lindsay, R., " On the Rounding-Up Process in High-Production Internal Grinding Machines By Digital Computer Simulation," Proc. of 12th Inter. M.T.D.R. Conf., p. 235.

34. Hahn, R. and Lindsay, R., " Factors Affecting Precision High Production Internal Grinding," SME, Manufacturing Engineering Trans. 1973. p. 57.

35. Tonshoff, H., Rohr, G. and Althaus, P., "Process Control in Internal Grinding," Annals of the CIRP Vol. 29/1, 1980. p. 207.

36. Kel'zon, A. and Guk'yamukhov, P., "Enternal Grinding By Spindles on Elastic Supports," Vestnik Mashinostroeniya, Vol. 63, Issue 8, 1983, p. 30.

37. Chien, A., " Centerless Plunge Feed with Additional High Friction Damping," Proc. M.T.D.R. 1975.

38. Richards, D., Rowe, W. and Koenigsberger, F., " Geometrical Configurations for stability in the Centerless Grinding Process,"

39. Trimal, G., " Comparison of Creep Feed and Conventional Grinding," Proc. of the 21st Inter. M.T.D.R. Conf. p. 323.

40. Hahn, R., " On the Universal Process Parameters Governing the Mutual Machining of Workpiece and Wheel Applied to the Creep-Feed Grinding Process," Annals of the CIRP Vol. 33/1, 1984. p. 189.

41. Matsuo, T., Matsubara, K. and Morita, T., " Influence of Working Parameters in Constant-Load Heavy Grinding," Annals of the CIRP, Vol. 32/1, 1983. p. 233.

42. Hahn, R., " The Influence of Threshold Forces on Size, Roundness and Contour Errors in Precision Grinding," Annals of the CIRP, Vol. 30/1, 1981. p. 251.

43. Hahn, R. and Lindsay, R., " Relationship Between Wheel Characteristics and Operating Problems in High-Production Precision Grinding," Proc. of 13th Inter. M.T.D.R. Conf.

44. Hahn, R., " On the Theory of Regenerative Chatter in Precision-Grinding Operations," Trans. of the ASME, May, 1954. p. 593.

45. Salje, E., Damios,H. and Teiwes, H., "Problems in Profile Grinding," Annals of the CIRP, 1981.

46. Kudinov, V., " Computer Aided Dynamics Calculations for Surface Grinders," Stankii Instrument, Vol. 45, Issue 11, 1974, p. 12.

47. Matsuo, T. and Sonoda, S., " The Rating of Wheels in Laboratory Snag Grinding," Annals of th CIRP, Vol. 29/1, 1981, p. 221.

48. Asada, H. and Goldfine, N. " Optimal Compliance Design for Grinding Robot Tool Holders," submitted to 1985 IEEE Conf. on Robotics and Automation.

49. Asada, H. and Goldfine, N. " Dynamic Analysis and Tool Holder Design for Grinding with Robots," submitted to 1985 American Controls Conf.

50. Peters, J., Snoeys, R. and Decneut, A., "The Proper Selection of Grinding Conditions in Cylindrical Plunge Grinding,"Proceedings: 16th International Machine Tool Design and Research Conference, MacMillan Press Ltd., Publishers.

51. Bhateja, C. and Lindsay, R., Grinding, Theory Techniques and Troubleshooting, SME Marketing Services Department, 1982.

52. Hahn, R. S., "Vibrations of Flexible Precision Grinding Spindles," Transactions ASME 1958, No. 59-A 97.

53. Gieseke, E., "Adaptive Constraint Control with Automatic Cut Segmentation for Turning," Diss RWTH, Aachen, 1973.